ON INTEGRAL REPRESENTATIONS OF FRACTIONAL BROWNIAN MOTION

LUKE COLIN THORBURN

Supervised by Prof. Konstantin Borovkov

Masters Thesis
May 2019

School of Mathematics and Statistics
The University of Melbourne

Time is deeply interlocking in this way.

– Sarah Perry, *After Temporality*

Acknowledgements

To Kostya, thank you for your generosity, rigour, tangential factoids, impersonation of the Gumbel distribution, and excellent choice of topic in which to spend eighteen months marinating. Thank you also to Barry Hughes, Klemens Fellner, Liam Carroll, Jesse Gelle-Redman and David Ridout for related conversations, and to Anna and my family for their patience and support throughout.

Contents

Notation

$:=$	defining equality	$\mathbb{1}(E)$	indicator of set/condition E
$\mathbf{P}$	probability	$\overline{E}$	closure of set E
$\mathbf{E}$	expectation	$\mathscr{B}(E)$	class of Borel subsets of E
$\searrow$	approach from above	$\mathsf{span}(E)$	linear span of vectors in E
$\nearrow$	approach from below	$\mathsf{det}(A)$	determinant of matrix A
$(\cdot)_+$	$\max\{\cdot, 0\}$	$\mathsf{diag}(\boldsymbol{a})$	diagonal matrix with elements of vector $\boldsymbol{a}$ on major diagonal
$(\cdot)_-$	$\max\{-\cdot, 0\}$	A'	transpose of matrix A
$\mathbb{N}$	natural numbers	$\mathbf{0}_n$	$n \times 1$ vector of zeroes
$\mathbb{R}_{\geqslant 0}$	$[0, \infty) \subset \mathbb{R}$	$\mathbf{1}_n$	$n \times 1$ vector of ones
$\mathbb{R}_{>0}$	$(0, \infty) \subset \mathbb{R}$	I_n	$n \times n$ identity matrix
MVN	multivariate normal distribution		
L^2	Hilbert space of square-integrable random variables		

∂_x^k	partial derivative $\frac{\partial^k}{\partial x^k}$	$\Gamma(\cdot)$	gamma function
$\delta_{\boldsymbol{x}}$	Dirac delta function at $\boldsymbol{x}$	$B(\cdot, \cdot)$	beta function
δ_{ij}	Kronecker's delta	$(a)_k$	Pochhammer symbol

$_2F_1$ Gauss hypergeometric function $_2F_1(a, b, c, z) := \sum_{k=0}^{\infty} \frac{(a)_k (b)_k}{(c)_k} \frac{z^k}{k!}$

$\overset{*}{B}{}_t^H$	the Mandelbrot-van Ness representation of fBm
$\widehat{B}_t^H$	the Molchan-Golosov representation of fBm
$\overline{B}_t^H$	the Muravlev representation of fBm
$\widetilde{B}_t^H$	Kolmogorov's spectral representation of fBm

Chapter 1

Introduction

Fractional Brownian motion (fBm) is a generalisation of the standard Brownian motion (Bm) to accommodate particular structures of dependency between disjoint increments. First described by Kolmogorov in 1940, fBm and its discrete analog, fractional Gaussian noise (fGn), are now widely used to model time series or spatial data that exhibit fractal properties. They and derivative processes have been used in bioengineering to model regional blood flow distributions in the heart, lungs and kidneys [2], in communication theory to model the arrivals of network packets [8], in hydrology to model water levels in rivers [31] and the hydraulic conductivity of soils [41], in finance to model the prices of financial instruments [6], in genetics to model stochastic gene expression [35] and DNA walks [1], in Bayesian machine learning to induce a prior distribution on the function space of regression curves [59], in computer graphics to generate natural-looking clouds, terrain and cellular noise [15], in soft matter physics to describe diffusion in crowded fluids [12], and in fluid dynamics to model the phase discrepancies along a turbulent wave-front [48].

Despite this breadth of applications, the analytical methods available for computing statistics of fBm models are limited by the fact that the process is neither Markov nor a semimartingale. A pool of structurally varied representations thus serves as an important resource. Representations of fBm in terms of the more familiar standard Brownian motion have been used to prove its existence, derive properties of sample paths, propose simulation and approximation algorithms [8], develop theories of stochastic integration with respect to fBm [7, 37], and facilitate various statistical results [43, 26]. In this thesis, two existing time domain integral representations of fBm are investigated.

First, the derivation of the Muravlev representation is presented in detail, and properties of the infinite-dimensional Ornstein-Uhlenbeck process appearing in its integrand are investigated, including the Markov property and the smoothness of its sample surfaces in the spatial direction. The means by which long-range dependence arises in an integral over short-range dependent processes is also discussed.

Second, geometric intuition for the Molchan-Golosov representation is developed, which can be viewed as a contortion of the helix formed by fBm in the Hilbert space of square-integrable random variables. In the discrete-time case, this geometric transformation is shown to be equivalent (in a sense made precise) to the premultiplication of a multivariate Gaussian vector consisting of fBm increments by a lower triangular matrix constructed via Cholesky factors. As the size of the mesh on which the fBm is discretised shrinks to zero, this finite-dimensional linear transformation is shown numerically to approach the Molchan-Golosov integral transformation.

The thesis has four main chapters. Chapter 2 outlines requisite background theory, including a construction of Itô integration on the half line. Chapter 3 summarises the literature on fBm representations. The Muravlev and Molchan-Golosov representations are discussed in Chapters 4 and 5, respectively. To close, some concluding remarks are made in Chapter 6.

Chapter 2

Preliminaries

2.1 The space L^2

The set of square-integrable random variables on a given probability space forms a Hilbert space. This perspective can sometimes provide useful geometric intuition for otherwise purely probabilistic arguments.

Formally, let $(\Omega, \mathcal{F}, \mathbf{P})$ be a probability space. Denote by $L^2(\Omega, \mathcal{F}, \mathbf{P})$ — or simply L^2 when the particulars of the underlying probability space are not relevant — the tuple $(V, \langle \cdot, \cdot \rangle_{L^2})$, where

$$V := \Big\{ X : \Omega \to \mathbb{R} \mid \mathbf{E}[X^2] < \infty \Big\} \,/\, \overset{\text{a.s.}}{=}$$

is the set of equivalence classes of almost surely equal random variables with finite second moments. In practice, we usually refer to the elements of L^2 as being random variables, rather than the strictly correct equivalence classes. Denoting by $[X]$ the equivalence class of random variables almost surely equal to X, the inner product and norm on L^2 are defined as follows:

$$\langle [X], [Y] \rangle_{L^2} := \mathbf{E} XY, \qquad \| [X] \|_{L^2} := \sqrt{\langle [X], [X] \rangle_{L^2}} = \sqrt{\mathbf{E}\{X^2\}}.$$

The space $L^2(\Omega, \mathcal{F}, \mathbf{P})$ is complete and thus forms a Hilbert space.

2.2 Process properties

In this section a number of distributional properties of stochastic processes are introduced.

Self-similarity

The following definition is modelled on that given in [52, Def 2.5.1].

Definition 2.1 (self-similarity)**.** A stochastic process $(X_t)_{t \in \mathbb{R}}$ is called *self-similar* if there exists $H > 0$ such that, for all $a > 0$,

$$(X_{at})_{t \in \mathbb{R}} \overset{d}{=} (a^H X_t)_{t \in \mathbb{R}}$$

where, when equating processes, $\overset{d}{=}$ denotes equality of the finite-dimensional distributions. The term *H-self-similar* is also used to refer to such a process.

Self-similar processes are important because, among other properties, they arise as the natural limits in functional central limit theorems, analogous to the role that stable distributions play in one-dimensional central limit theorems [28].

Stationarity of increments

The following two notions are standard; these definitions follow [9, p.99] with a slight modification of terminology.

Definition 2.2 (strictly stationary increments)**.** A stochastic process $(X_t)_{t\geqslant 0}$ has *strictly stationary increments* if, for any $h > 0$,

$$(X_{t+h} - X_h)_{t\geqslant 0} \stackrel{d}{=} (X_t - X_0)_{t\geqslant 0}.$$

Definition 2.3 (weakly stationary increments)**.** A stochastic process $(X_t)_{t\geqslant 0}$ has *weakly stationary increments* if, for any $s, t \geqslant 0$, $\mathbf{E}[(X_t - X_s)^2]$ depends only on $|t-s|$.

Long-range dependence

There are at least five distinct definitions of long-range dependence used in the literature, see [52, Ch. 2] for a comprehensive survey. Here, we define long-range dependence of a weakly stationary process to be a property of its autocovariance function. The *autocovariance function* of discrete-time, weakly stationary process $(X_n)_{n\in\mathbb{N}}$ is the function γ_X defined by

$$\gamma_X(n) := \mathbf{E}X_{n+1}X_1 - \mathbf{E}X_{n+1}\mathbf{E}X_1, \qquad n \in \mathbb{N}.$$

Definition 2.4 (long-range dependence)**.** A discrete-time process $(X_n)_{n\in\mathbb{N}}$ is *long-range dependent* if its autocovariances are not absolutely summable. That is, if the series

$$\sum_{k=1}^{\infty} |\gamma_X(k)|$$

diverges. A process is *short-range dependent* if it is not long-range dependent.

This is the third definition from [52, Ch. 2]. Note that saying a process is long-range dependent is not merely saying that there exist non-zero covariances between random variables in the sequence separated by arbitrarily large time intervals, but that the magnitude of such covariances decay sufficiently slowly as the length of the intervening time interval increases.

For our purposes, we will say a continuous-time, weakly stationary process $(X_t)_{t\in\mathbb{R}_{\geqslant 0}}$ is long-range dependent if the discrete-time process $(X_n - X_{n-1})_{n\in\mathbb{N}}$ of its increments is long-range dependent. If X_t is a continuous-time process, the notation γ_X will refer to the autocovariance function of its corresponding increment process.

Long-range dependent processes and self-similar processes are related. Specifically, if $(X_t)_{t\in\mathbb{R}_{\geqslant 0}}$ is H-self-similar for some $H \in (1/2, 1)$ with strictly stationary increments, then $(X_n - X_{n-1})_{n\in\mathbb{N}}$ will be long-range dependent [52, Prop. 2.8.1].

Markovity

In qualitative terms, a Markov process (or a process that has the *Markov property*) is one for which the distribution of the future trajectory of the process given its history up to time t depends only on the value of the process at time t. To make this notion sufficiently precise for our purposes, we use a simplified version of the definition given by Gikhman and Skorohod [27, Ch. 1 §3]. Let

- $(\Omega, \mathcal{F})$ be a measurable space (the sample space) equipped with a family $\{\mathcal{F}_t \mid t \in \mathbb{R}_{\geqslant 0}\}$ (or just $\mathcal{F}_t$) of sub-σ-algebras of $\mathcal{F}$ such that if $s \leqslant t$ then $\mathcal{F}_s \subseteq \mathcal{F}_t$ (a filtration);
- $(\Xi, \mathcal{E})$ be another measurable space (the space in which the process takes its values);
- $X : \mathbb{R}_{\geqslant 0} \times \Omega \to \Xi$ be a function (the process); and
- $\{P_{s,x} \mid s \in \mathbb{R}_{\geqslant 0}, x \in \Xi\}$ (or just $P_{s,x}$) be a collection of probability measures on the σ-algebra generated by $\cup_{t \geqslant s} \mathcal{F}_t$.

Definition 2.5 (Markov process)**.** The triple $(X_t, \mathcal{F}_t, P_{s,x})$ is called a *Markov process* if it satisfies the following properties:

M1 For all $t \in \mathbb{R}_{\geqslant 0}$, the map $X_t : \Omega \to \Xi$ which takes $\omega \mapsto X(t, \omega)$ is $\mathcal{F}_t$-measurable.

M2 For all $E \in \mathcal{E}$ and $s, t \in \mathbb{R}_{\geqslant 0}$ such that $s \leqslant t$, the function $x \mapsto P_{s,x}(\{X_t \in E\})$ is $\mathcal{E}$-measurable.

M3 For all $x \in \Xi$ and $s \in \mathbb{R}_{\geqslant 0}$, $P_{s,x}(\{X_s \in \Xi \setminus x\}) = 0$.

M4 (Markov property) For all $x \in \Xi$, $E \in \mathcal{E}$ and $r, s, t \in \mathbb{R}_{\geqslant 0}$ such that $r \leqslant s \leqslant t$, the probability $P_{r,x}(\{X_t \in E | \mathcal{F}_s\}) = P_{s,X_s}(\{X_t \in E\})$.

Semimartingale

Definition 2.6 (semimartingale)**.** A stochastic process $(X_t)_{t \geqslant 0}$ is a *semimartingale* if there exists a decomposition

$$X_t = M_t + A_t,$$

where $(M_t)_{t \geqslant 0}$ is a local martingale, and $(A_t)_{t \geqslant 0}$ is a cádlág adapted process with locally bounded variation.

Semimartingales are important because they are the broadest family of processes with respect to which Itô integrals, introduced in Section 2.4, can be constructed (see [53] for the general theory).

Gaussianity

Definition 2.7 (Gaussian process)**.** A *Gaussian process* is a stochastic process for which all the finite-dimensional distributions are (multivariate) Gaussian.

Gaussian processes can be convenient to work with because they are uniquely specified by their mean and covariance functions. Two key examples will appear frequently in this thesis.

- The *standard Brownian motion* (Bm) on the half line is a mean-zero Gaussian process $(B_t)_{t\in\mathbb{R}_{\geqslant 0}}$ with covariance function given by:

  $$\mathbf{E}[B_s B_t] = \min\{s,t\} \qquad \text{for } s,t\in\mathbb{R}_{\geqslant 0}.$$

  Disjoint increments of a standard Bm are independent, and the sample paths of the process can be constructed to be (surely) continuous. Often we will make use of a Bm on the real line, which is a stochastic process $(B_t)_{t\in\mathbb{R}}$ constructed by

  $$B_t := \begin{cases} B^1_t, & \text{if } t\geqslant 0, \\ B^2_{-t}, & \text{if } t<0 \end{cases},$$

  where $(B^1_t)_{t\in\mathbb{R}_{\geqslant 0}}$, $(B^2_t)_{t\in\mathbb{R}_{\geqslant 0}}$ are independent standard Brownian motions on the half line.

- The *Ornstein-Uhlenbeck process* is, for any $\beta\in\mathbb{R}_{>0}$, a mean-zero Gaussian process $(Z^\beta_t)_{t\in\mathbb{R}_{\geqslant 0}}$ with covariance function given by:

  $$\mathbf{E}[Z^\beta_s Z^\beta_t] = \frac{1}{2\beta}e^{-\beta(t-s)} \qquad \text{for } s,t\in\mathbb{R}_{\geqslant 0},\ s\leqslant t.$$

The above definitions are standard but and be found, for instance, in [52, Sec. 1.1.1]. Both processes can have their parameter sets truncated to bounded intervals without unexpected consequences.

2.3 Fractional Brownian motion

The focus of this thesis is another family of Gaussian processes.

Definition 2.8 (fractional Brownian motion)**.** For any $H\in(0,1]$, the *fractional Brownian motion with Hurst parameter H* (H-fBm) is defined to be a mean-zero Gaussian process $B^H_t = (B^H_t)_{t\geqslant 0}$ with covariance function given by:

$$\mathbf{E}[B^H_s B^H_t] = \frac{1}{2}(s^{2H}+t^{2H}-|s-t|^{2H}) \qquad \text{for all } s,t\in\mathbb{R}_{\geqslant 0}. \tag{2.1}$$

The covariance function can indirectly but more elegantly be specified by setting $B^H_0 := 0$ and, for $s,t\geqslant 0$, $\|B^H_t - B^H_s\|_{L^2} := |t-s|^H$.

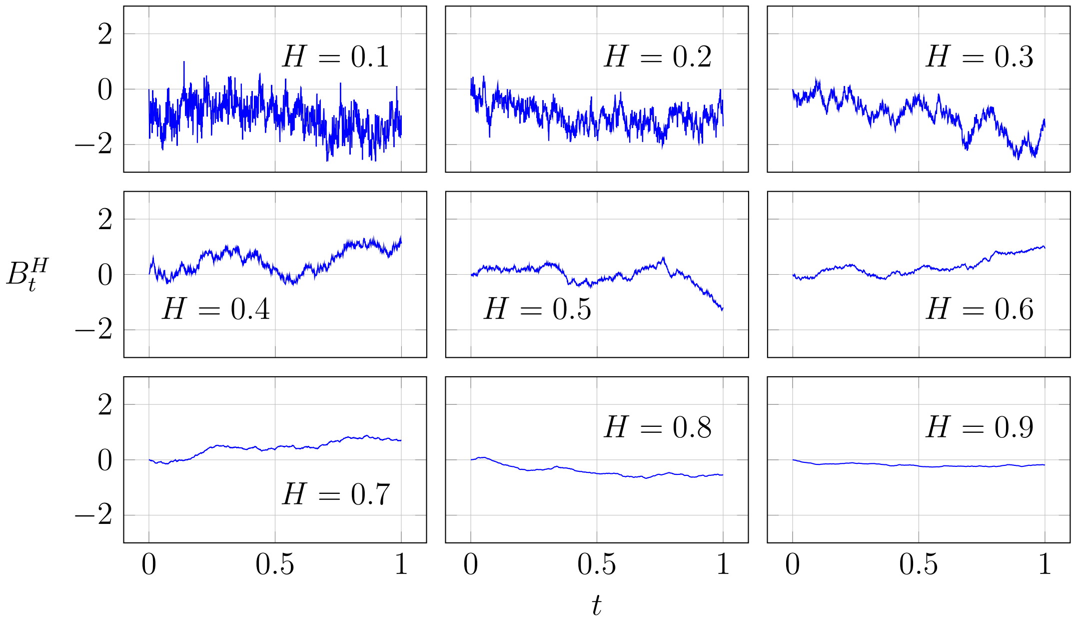

Figure 2.1: Simulated sample paths of fractional Brownian motions at particular Hurst parameters. Each path is simulated on a grid of time parameters, $t = 0.001k$ for $k \in \mathbb{N}_{\leqslant 1000}$.

The Hurst parameter $H \in (0, 1]$ controls the correlation of disjoint increments, which is positive for $H \in (1/2, 1]$ and negative for $H \in (0, 1/2)$. At $H = 1/2$, the process is the standard Brownian motion B_t with independent increments. Sample fBm paths for a range of Hurst parameters are shown in Figure 2.1.

When $H = 1$, the process trajectory is a straight line with random slope—namely, $B_t^H = tB_1^H$ almost surely. As $H \searrow 0$, the process converges in the sense of convergence of finite-dimensional distributions to a white noise process with random initial displacement. Specifically, if $(W_t)_{t\in\mathbb{R}_{\geqslant 0}}$ is a stochastic process for which each W_t is an independent standard normal random variable, then as $H \searrow 0$ the finite-dimensional distributions of $(B_t^H)_{t\in\mathbb{R}_{\geqslant 0}}$ converge to those of the process $((W_t - W_0)/\sqrt{2})_{t\in\mathbb{R}_{\geqslant 0}}$. This fact was proved in [3, Sec. 4].

Several key properties of fBm are stated below.

Proposition 2.1. *The process $(B_t^H)_{t\geqslant 0}$ is H-self-similar.*

Proof. For any $a > 0$, the processes $(B_{at}^H)_{t\geqslant 0}$ and $(a^H B_t^H)_{t\geqslant 0}$ are both mean-zero, Gaussian. Moreover, they have identical coveriance functions, because for $s, t \geqslant 0$,

$$\begin{aligned}\mathbf{E}B_{as}^H B_{at}^H &= \frac{1}{2}\Big((at)^{2H} + (as)^{2H} - |at - as|^{2H}\Big)\\ &= \frac{a^{2H}}{2}(t^{2H} + s^{2H} - |t - s|^{2H}) = \mathbf{E}(a^H B_t^H)(a^H B_s^H).\end{aligned}$$

Gaussian processes are fully specified by their mean and covariance functions, so $(B_{at}^H)_{t\geqslant 0} \overset{d}{=} (a^H B_t^H)_{t\geqslant 0}$ and, thus, $(B_t^H)_{t\in\mathbb{R}_{\geqslant 0}}$ is H-self-similar. □

Proposition 2.2. *The process $(B_t^H)_{t\geqslant 0}$ has strictly stationary increments.*

Proof. Since the process is Gaussian, the distribution of each increment is fully described by its mean and covariance, so it is sufficient to note that for any $h > 0$ and $t \in \mathbb{R}_{\geqslant 0}$, the mean $\mathbf{E}[B^H_{t+h} - B^H_h] = 0$ and the variance

$$\mathbf{E}[(B^H_{t+h} - B^H_h)^2] = |t + h - h|^{2H} = |t|^{2H}$$

are both independent of h. □

These above two properties provide an alternative characterisation of an H-fBm which, up to a multiplicative constant, is the only Gaussian process which is H-self-similar and has stationary increments (see [52, Def. 2.6.2]).

Proposition 2.3. $(B^H_t)_{t\geqslant 0}$ *is long-range dependent if and only if* $H \in (1/2, 1]$.

The following proof is modelled on that in [21, Lem. 2.4].

Proof. Using the covariance function (2.1) of an H-fBm, we see that the autocovariance function of its increment process is

$$\begin{aligned}\gamma_{B^H}(n) &= \mathbf{E}[(B^H_{n+1} - B^H_n)(B^H_1 - B^H_0)] \\ &= \frac{1}{2}\left[(n+1)^{2H} - n^{2H} - \left(n^{2H} - (n-1)^{2H}\right)\right], \qquad \text{for } n \in \mathbb{N}.\end{aligned}$$

By applying the mean value theorem twice, γ_{B^H} can be shown to have the form

$$\gamma_{B^H}(n) = H(2H-1)(n + \theta_{H,n})^{2H-2} \qquad \text{for } n \in \mathbb{N},$$

where $\theta_{H,n} \in (-1, 1)$ for all possible H, n. Thus, the absolute sum of the autocovariances can be bounded as follows:

$$\sum_{n=1}^{\infty} |\gamma_{B^H}(n)| \begin{cases} \leqslant H|2H-1| \left((1+\theta_{1,H})^{2H-2} + \sum_{n=1}^{\infty} n^{2H-2}\right), & \text{if } H \in (0, 1/2), \\ \geqslant H|2H-1| \sum_{n=2}^{\infty} n^{2H-2}, & \text{if } H \in (1/2, 1]. \end{cases}$$

The p-series on the right-hand side converge and diverge respectively for the cases $H \in (0, 1/2)$ and $H \in (1/2, 1]$, so an H-fBm is long-range dependent if and only if $H \in (1/2, 1]$. □

Proposition 2.4. *If* $H \neq 1/2$, *then* $(B^H_t)_{t\geqslant 0}$ *is not a Markov process.*

Proposition 2.5. *If* $H \neq 1/2$, *then* $(B^H_t)_{t\geqslant 0}$ *is not a semimartingale.*

The preceeding two properties often mean that, relative to standard Bm, computations involving fBm with Hurst parameter $H \neq 1/2$ are typically more difficult. Proofs of Lemmas 2.4 and 2.5 can be found in [46, Thm. 2.2, 2.3].

Details on the history of fBm literature can be found in [21, 37, 39, 56].

2.4 Itô calculus

In this section the Itô integral on the half-line is constructed. The method used is a generalisation of that given in [47, Ch. 3].

Fix $t \in \mathbb{R}$. Take $(\Omega, \mathcal{F}, \{\mathcal{F}_s\}_{s\in(-\infty,t]}, \mathbf{P})$ to be a filtered probability space. On top of this underlying space, two additional spaces are built. The first is the Hilbert space $L^2 = L^2(\Omega, \mathcal{F}, \mathbf{P})$ as defined in Section 2.1. The second is the inner product space $\mathcal{Y}$ consisting of stochastic processes $(Y_s)_{s\in(-\infty,t]}$,

$$\begin{aligned} Y_s : \Omega &\to \mathbb{R} \\ \omega &\mapsto Y_s(\omega) \end{aligned}$$

such that the following three properties hold:

i. The map $(s, \omega) \mapsto Y_s(\omega)$ is $(\mathscr{B}((-\infty, t]) \times \mathcal{F})$-measurable;

ii. The process $(Y_s)_{s\in(-\infty,t]}$ is $\mathcal{F}_s$-adapted; and

iii. $\mathbf{E}\left[\int_{-\infty}^{t} Y_s^2 \, ds\right] < \infty$.

The inner product on $\mathcal{Y}$ is defined to be

$$\langle U_s, V_s \rangle_{\mathcal{Y}} := \int_{-\infty}^{t} \mathbf{E}[U_s V_s] \, ds,$$

and the norm $\|U_s\|_{\mathcal{Y}} := \langle U_s, U_s \rangle_{\mathcal{Y}}^{1/2}$. Let $(B_s)_{s\in\mathbb{R}}$ be a standard Bm on the real line with domain Ω, such that B_s is $\mathcal{F}_s$-adapted and, for all $s, t \in \mathbb{R}_{\geqslant 0}$ with $s < t$, the increment $B_t - B_s$ is independent of $\mathcal{F}_s$. For all $(Y_s)_{s\in(-\infty,t]} \in \mathcal{Y}$ we wish to define the following integral:

$$\mathcal{I}[Y_s] := \int_{-\infty}^{t} Y_s \, dB_s \, .$$

Initially, we define the integral for simple processes.

Definition 2.9 (simple process)**.** A stochastic process $(U_s)_{s\in(-\infty,t]} \in \mathcal{Y}$ is *simple* if it has the form

$$U_s = X_1 \mathbb{1}(s = s_1) + \sum_{i=1}^{N} X_i \mathbb{1}(s \in (s_i, s_{i+1}]),$$

for some increasing sequence of times $u = s_1 < \cdots < s_N = v$ (where $u, v \in (-\infty, t]$ and $N \in \mathbb{N}$) and some sequence of random variables $(X_i)_{i=1}^{N}$ such that X_i is $\mathcal{F}_{s_i}$-measurable.

Let $(U_s)_{s\in(-\infty,t]} \in \mathcal{Y}$ be a simple process as defined in Definition 2.9. The Itô integral of $(U_s)_{s\in(-\infty,t]}$ is defined as follows:

$$\int_{-\infty}^{t} U_s \, dB_s = \int_{u}^{v} U_s \, dB_s := \sum_{i=1}^{N} X_i (B_{s_{i+1}} - B_{s_i}).$$

Theorem 2.1 (Itô isometry for simple processes). *If $(U_s)_{s\in(-\infty,t]} \in \mathcal{Y}$ is simple, then $\|\mathcal{I}[U_s]\|_{L^2} = \|U_s\|_{\mathcal{Y}}$.*

Proof. First, note that if $\Delta B_i := B_{s_{i+1}} - B_{s_i}$, then

$$\mathbf{E}[X_i X_j \Delta B_i \Delta B_j] = \begin{cases} \mathbf{E}[X_i^2](s_{i+1} - s_i) & i = j \\ 0 & i \neq j \end{cases}. \tag{2.2}$$

This is because ΔB_i is independent of $\mathcal{F}_{s_i}$. Thus

$$\begin{aligned} \|\mathcal{I}[U_s]\|_{L^2}^2 &= \mathbf{E}\left[\left(\int_u^v U_s \, dB_s\right)^2\right] = \mathbf{E}\left[\left(\sum_{i=1}^N X_i (B_{s_{i+1}} - B_{s_i})\right)^2\right] \\ &\overset{(2.2)}{=} \sum_{i=1}^N \mathbf{E}[X_i^2](s_{i+1} - s_i) = \int_u^v \mathbf{E}[U_s^2] \, ds \\ &= \mathbf{E}\left[\int_u^v U_s^2 \, ds\right] = \|U_s\|_{\mathcal{Y}}. \end{aligned}$$

□

We can now proceed to construct the Itô integral for all $Y_t \in \mathcal{Y}$ via two steps.

Step 1. *Let V_s be an element of $\mathcal{Y}$ which is almost surely zero off a compact interval $[u, t]$ for some $u \in (-\infty, t)$. Then there exists a sequence of simple processes $(U_s^n)_{n=1}^\infty$ such that $U_s^n \to V_s$ in $\mathcal{Y}$.*

See [47, p.27] for the proof.

Step 2. *Let Y_s be an arbitrary element of $\mathcal{Y}$. Then there exists a sequence of processes $(V_s^n)_{n=1}^\infty$ almost surely zero off a compact interval (dependent on n) such that $V_s^n \to Y_s$ in $\mathcal{Y}$.*

Proof. Choose $V_s^n := Y_s \mathbb{1}(s \geqslant -n)$. Then

$$\begin{aligned} \|Y_s - V_s^n\|_{\mathcal{Y}} &= \mathbf{E}\left[\int_{-\infty}^t (Y_s - Y_s \mathbb{1}(s \geqslant u))^2 \, ds\right] \\ &= \mathbf{E}\left[\int_{-\infty}^t Y_s^2 \mathbb{1}(s < u) \, ds\right] \\ &= \mathbf{E}\left[\int_{-\infty}^t Y_s^2 - Y_s^2 \mathbb{1}(s \geqslant u) \, ds\right] \\ &= \mathbf{E}\left[\int_{-\infty}^t Y_s^2 \, ds\right] - \mathbf{E}\left[\int_{-\infty}^t Y_s^2 \mathbb{1}(s \geqslant u) \, ds\right] \xrightarrow{u \to -\infty} 0, \end{aligned}$$

because for $u_1 > u_2$,

$$0 \leqslant \int_{-\infty}^t Y_s^2 \mathbb{1}(s \geqslant u_1) \, ds \leqslant \int_{-\infty}^t Y_s^2 \mathbb{1}(s \geqslant u_2) \, ds \leqslant \int_{-\infty}^t Y_s^2 \, ds \quad \text{a.s.},$$

and so as $u \to -\infty$,

$$\mathbf{E}\left[\int_{-\infty}^t Y_s^2 \mathbb{1}(s \geqslant u) \, ds\right] \to \mathbf{E}\left[\int_{-\infty}^t Y_s^2 \, ds\right],$$

by the monotone convergence theorem. □

Definition 2.10 (Itô integral)**.** Let Y_s be an arbitrary element of $\mathcal{Y}$. Choose, via Steps 1 and 2, a sequence of simple processes $(U_s^n)_{n=1}^{\infty}$ such that $U_s^n \to Y_s$ in $\mathcal{Y}$. Then define

$$\int_{-\infty}^{t} Y_s \, dB_s := \lim_{n\to\infty} \int_{-\infty}^{t} U_s^n \, dB_s \tag{2.3}$$

where the limit is taken in L^2.

The limit exists because the sequence $(U_s^n)_{n=1}^{\infty}$ converges in $\mathcal{Y}$, so is Cauchy. The Itô isometry (Theorem 2.1) implies that the sequence of Itô integrals in (2.3) is also Cauchy in the Hilbert space L^2, so converges to a limit in L^2.

The Itô isometry also extends to the general case.

Theorem 2.2 (Itô isometry)**.** *If $Y_s \in \mathcal{Y}$, then $\|\mathcal{I}[Y_s]\|_{L^2} = \|Y_s\|_{\mathcal{Y}}$.*

For a process $(X_t)_{t\in\mathbb{R}}$ that satisfies

$$X_t - X_u = \int_u^t \mu(s)\, ds + \int_u^t \sigma(s)\, dB_s, \qquad \text{for all } u \in \mathbb{R}_{\leqslant t} \cup \{-\infty\},$$

where μ, σ are stochastic processes sufficiently well-behaved for the integrals to exist, it is standard in stochastic calculus to adopt the shorthand differential form

$$dX_t = \mu(t)\, dt + \sigma(t)\, dB_t\,.$$

An important example for this thesis is the previously-introduced Ornstein-Uhlenbeck process $(Z_t^\beta)_{t\in\mathbb{R}}$, which satisifies the so-called Langevin stochastic differential equation:

$$dZ_t^\beta = -\beta Z_t^\beta\, dt + dB_t\,.$$

This form makes plain that the Ornstein-Uhlenbeck process is similar to a standard Bm but has an extra 'mean-reverting' term $-\beta Z_t^\beta\, dt$ which manifests as a tendency for the process to return to zero. The strength of the tendency increases proportionally to the amount by which the process deviates from zero.

Later, we will also require the following standard result.

Theorem 2.3 (Itô formula)**.** *Let $(X_t)_{t\in\mathbb{R}}$ be a stochastic process satisfying*

$$dX_t = \mu(t)\, dt + \sigma(t)\, dB_t,$$

and let $g(t,x) : \mathbb{R}^2 \to \mathbb{R}$ be a function that is twice continuously differentiable in x and once continuously differentiable in t. Then if $Y_t := g(t, X_t)$, the process $(Y_t)_{t\in\mathbb{R}}$ satisfies the formula

$$dY_t = \partial_t g(t, X_t)\, dt + \partial_x g(t, X_t)\, dX_t + \frac{1}{2}\partial_x^2 g(t, X_t)(dX_t)^2,$$

where $(dX_t)^2 = dX_t \cdot dX_t$ is computed according to the rules

$$dt \cdot dt = dt \cdot dB_t = 0, \text{ and } dB_t \cdot dB_t = dt\,.$$

A proof can be found in [47, Thm. 4.1.2].

Chapter 3

Literature review

There are a number of known representations of fBm in terms of other processes, most commonly standard Brownian motion via an Itô integral. This chapter is a non-exhaustive review of the most prominent, their connections to other representations, and some applications.

3.1 Representations

3.1.1 Time domain

Mandelbrot-van Ness

The following representation was introduced in the seminal 1968 paper of Mandelbrot and van Ness [30, Def. 2.1].

Theorem 3.1 (Mandelbrot-van Ness representation). *Let $H \in (0,1)$ and $(B_t)_{t\in\mathbb{R}}$ be a standard Bm on the real line. If*

$$\overset{*}{B}{}_t^H := \overset{*}{c}_H \int_{\mathbb{R}} \left((t-s)_+^{H-1/2} - (-s)_+^{H-1/2} \right) dB_s, \tag{3.1}$$

where $(\cdot)_+ = \max\{\cdot, 0\}$ and the constant

$$\overset{*}{c}_H = \left(\int_0^\infty \left((1+s)^{H-1/2} - s^{H-1/2} \right)^2 ds + \frac{1}{2H} \right)^{-\frac{1}{2}} = \frac{[\Gamma(2H+1)\sin(\pi H)]^{\frac{1}{2}}}{\Gamma(H+1/2)},$$

then $(\overset{*}{B}{}_t^H)_{t\in\mathbb{R}_{\geqslant 0}}$ is an H-fBm.

See [46, Prop. 2.3] for a proof. The name *fractional Brownian motion* was coined by Mandelbrot and van Ness as a result of this integral representation, the integrand of which can be expressed as a fractional integral. See [50] and [21, Ch. 4] for an introduction to fractional calculus and its connections with fBm.

Remark. Note that the constant $\overset{*}{c}_H$ quoted here is different from that given in [30], which results in a similar process with a covariance function which differs from (2.1) by a constant factor. See [37, App. A] for a computation of the correct constant.

Theorem 3.1 is sometimes referred to as a 'moving average' representation because it specifies the value B_t^H as a weighted average over the process $(B_s)_{s\leqslant t}$, with the integrand determining the weight given to different regions of the standard Bm driver. Figure 3.1 shows how the weights vary in H and s.

In econometrics, the process given by (3.1) is known as *Type I* fBm [32]. So-called *Type II* fBm is a different but related process given by discarding part of the integrand in (3.1), more commonly known as *Riemann-Liouville type* fBm [30, Ch. 2].

CONNECTIONS. Several generalisations of the Mandelbrot-van Ness (MvN) representation are known, revealing that it is one of a class of structurally similar integral representations of fBm. For example, it is noted in [55, Eq. 7.2.7] that for $(\cdot)_- = \max\{-\cdot, 0\}$ and any $a, b \in \mathbb{R}$,

$$\int_{\mathbb{R}} \left[a\left((t-s)_+^{H-1/2} - (-s)_+^{H-1/2}\right) + b\left((t-s)_-^{H-1/2} - (-s)_-^{H-1/2}\right)\right] dB_s \tag{3.2}$$

specifies an H-fBm up to a multiplicative constant. A similar generalisation in terms of cusp functions is given in [26]. Additionally, Jost [20, Remark 5.10] points out that truncating the lower terminal of integration to some finite value does not alter the covariance of the representation. While it is clear that (3.1) is not a structurally unique representation, it is shown in [16] that for $H \in [1/2, 1)$ and ϕ falling within a particular class of functions, it is the only integral of the form

$$\int_{\mathbb{R}} (\phi(t-s) - \phi(s))\, dB_s$$

that specifies an H-fBm.

Additionally, the Mandelbrot-van Ness representation has been generalised to a transformation formula, see (3.7).

The Muravlev representation (3.5) is derived from the Mandelbrot-van Ness representation.

APPLICATIONS. In addition to serving as a starting point for the derivation of other representations as outlined above, the Mandelbrot-van Ness representation is used in the definition of Wiener integration with respect to fBm [37, Ch. 1.6].

Molchan-Golosov

The following representation is widely useful because it represents an H-fBm as a stochastic integral over the compact interval $[0, t]$.

Theorem 3.2 (Molchan-Golosov representation)**.** *Let $H \in (0,1)$, and $(B_t)_{t\in\mathbb{R}_{\geqslant 0}}$ be a standard Bm. If*

$$\widehat{B}_t^H := \widehat{c}_H \int_0^t (t-s)^{H-1/2} {}_2F_1\left(1/2 - H, H - 1/2, H + 1/2, \frac{s-t}{s}\right) dB_s, \tag{3.3}$$

where ${}_2F_1$ is the Gauss hypergeometric function and the constant

$$\widehat{c}_H = \frac{[\Gamma(2H+1)\sin(\pi H)]^{\frac{1}{2}}}{\Gamma(H + 1/2)},$$

then $(\widehat{B}_t^H)_{t\in\mathbb{R}_{\geqslant 0}}$ is an H-fBm.

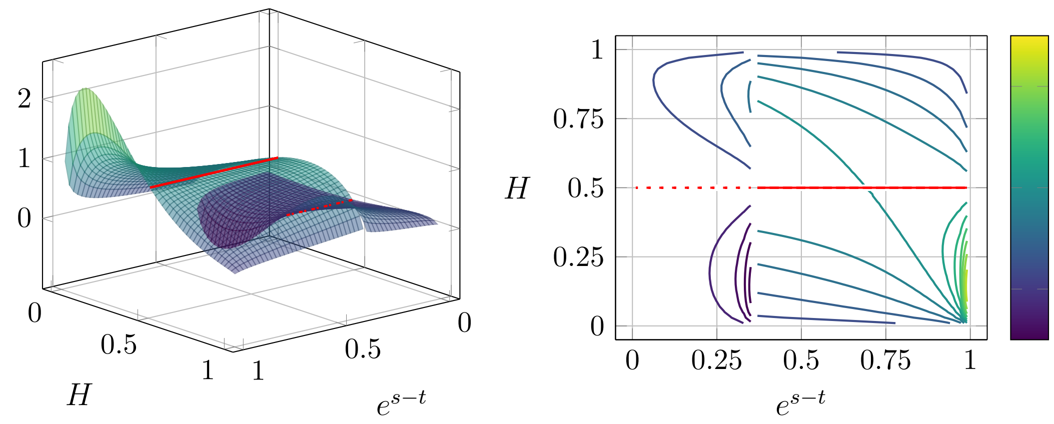

Figure 3.1: The integrand $\overset{*}{c}_H \left((t-s)_+^{H-1/2} - (-s)_+^{H-1/2}\right)$ appearing in the Mandelbrot-van Ness representation of an H-fBm for fixed $t = 1$, evaluated on a grid: $e^{s-t} = 0.01+0.02(k-1)$ for $k \in \mathbb{N}_{\leqslant 50}$, and $H = 0.01 + 0.02(k-1)$, for $k \in \mathbb{N}_{\leqslant 50}$. Note the discontinuity at $s = 0$. In the case of $H = 1/2$, the integrand is equal to $\mathbb{1}(s > 0)$ (the red line), reducing the stochastic integral to its standard Bm driver. The peak near $(s, H) = (t, 0)$ corresponds to the increased roughness of the sample paths as $H \searrow 0$, and the trough near $(s, H) = (0, 0)$ corresponds to the random initial displacement of the white noise process which arises in the limit as $H \searrow 0$.

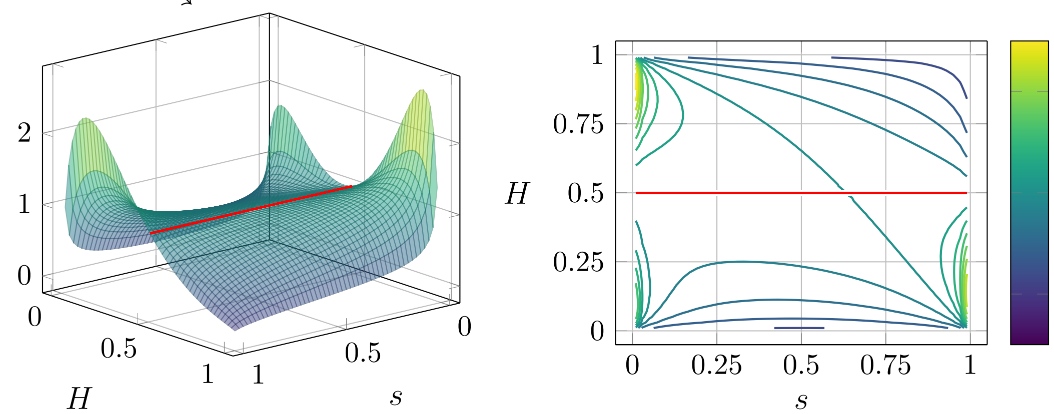

Figure 3.2: The integrand $\widehat{c}_H (t-s)^{H-1/2} {}_2F_1(1/2 - H, H - 1/2, H + 1/2, (s-t)/s)$ appearing in the Molchan-Golosov representation of an H-fBm for fixed $t = 1$, evaluated on a grid: $s = 0.01 + 0.02(k-1)$ for $k \in \mathbb{N}_{\leqslant 50}$, and $H = 0.01 + 0.02(k-1)$, for $k \in \mathbb{N}_{\leqslant 50}$. In the case of $H = 1/2$, the integrand is identically 1, reducing the stochastic integral to its standard Bm driver. The peaks near $(s, H) = (t, 0)$ and $(s, H) = (0, 0)$ have the same interpretations as the corresponding extrema in Figure 3.1. The additional peak near $(s, H) = (0, 1)$ corresponds to the long-range dependence of the process when $H \in (1/2, 1)$.

Several sources imply the representation follows from the 1969 work of Molchan and Golosov [40], but a much clearer proof is given in [21, Thm. 3.1]. In [45], the representation is derived for the case $H \in (1/2, 1)$ via an elementary approach.

Note that the expression for the constant $\widehat{c}_H$ given here differs from that given in [21, Lem. 3.2], in order to emphasise that $\widehat{c}_H = \overset{*}{c}_H$, the constant from the Mandelbrot-van Ness representation. The expression used in [21, Lem. 3.2] can be obtained using the reflection relation

$$\Gamma(1-z)\Gamma(z) = \frac{\pi}{\sin(\pi z)}, \qquad \text{if } z \in \mathbb{C} \setminus \mathbb{Z}_{\leqslant 0},$$

and the Legendre duplication formula

$$\Gamma(z)\Gamma(z + 1/2) = 2^{1-2z}\sqrt{\pi}\,\Gamma(2z), \qquad \text{if } z \in \mathbb{C} \setminus \mathbb{Z}_{\leqslant 0}.$$

These can respectively be found, for example, in [58, (1)] and [57, (50)].

As for the Mandelbrot-van Ness representation, the Molchan-Golosov representation can be thought of as a moving average and visualising the integrand in (3.3) provides some intuition for how the moving average weights different regions of the standard Bm driver to obtain an H-fBm. The integrand is plotted in Figure 3.2.

The dependence of the integrand on t implies fBm is not an Itô process, but it is a *Volterra process*, a term applied to stochastic processes that have the form

$$\int_0^t f(s,t)\, dB_s,$$

for some deterministic function f such that the integral exists. A concise introduction to Volterra processes can be found in [21, Ch. 6].

That such a finite-time interval representation of fBm exists, follows from the fact that fBm is the simplest example of a *Hermite process*, as it is known that all Hermite processes have finite time interval representations. See [51, Thm. 1.1] for the definition of a Hermite process and general formulae for such representations.

CONNECTIONS. The Mandelbrot-van Ness representation can be derived as a boundary case of an appropriately time-shifted Molchan-Golosov transformation formula (see Theorem 3.6). The proof, however, is quite involved — see [22] for details.

The Molchan-Golosov representation has also been generalised to a transformation formula, see Theorem 3.6.

APPLICATIONS. Jost [21, Rem. 3.3] provides a concise summary of the numerous results for fBm which are based on the Molchan-Golosov representation, which include a Girsanov fomula [45, Thm. 4.1], a Lévy characterisation [38], and a prediction formula [50, Ch. 8]. It is also used to define a stochastic integral with respect to fBm via Malliavin calculus [7].

Muravlev

The following representation is much more recent. Partial results for the cases $H \in (0, 1/2)$ and $H \in (1/2, 1)$ were published in [4] and [5, Sec. 2], respectively, in the late 1990s. The version stated here appeared in 2011 [43, Cor. 1], and was obtained by Muravlev without knowledge of the earlier work.

Theorem 3.3 (Muravlev representation)**.** *Let $H \in (0, 1/2) \cup (1/2, 1)$ and $(B_t)_{t\in\mathbb{R}}$ be a standard Bm on the real line. For each $\beta \in \mathbb{R}_{>0}$, let $(Z_t^\beta)_{t\in\mathbb{R}_{\geqslant 0}}$ be the Ornstein-Uhlenbeck process given by the following expression*

$$Z_t^\beta = e^{-\beta t} \int_{-\infty}^{t} e^{\beta s}\, dB_s \,. \tag{3.4}$$

If

$$\overline{B}_t^H = \begin{cases} \overline{c}_H \int_0^\infty \beta^{-1/2-H}(Z_t^\beta - Z_0^\beta)\, d\beta, & \text{if } H \in (0, 1/2)\,, \\ \overline{c}_H \int_0^\infty \beta^{-1/2-H}(Z_t^\beta - Z_0^\beta - B_t)\, d\beta, & \text{if } H \in (1/2, 1)\,, \end{cases} \tag{3.5}$$

where the constant

$$\overline{c}_H = \frac{[\Gamma(2H+1)\sin(\pi H)]^{1/2}}{B(1/2 + H, 1/2 - H)},$$

then $(\overline{B}_t^H)_{t\in\mathbb{R}_{\geqslant 0}}$ is an H-fBm.

The representation can be derived from the Mandelbrot-van Ness representation [43]. A direct computation of the covariance function does not appear to have been published.

Note that in [43, Cor. 1], Muravlev uses an equivalent specification of $(Z_t^\beta)_{t\in\mathbb{R}_{\geqslant 0}}$, namely:

$$Z_t^\beta = e^{-\beta t}\xi_\beta + e^{-\beta t} \int_0^t e^{\beta s}\, dB_s,$$

where $(\xi_\beta)_{\beta\in\mathbb{R}_{>0}}$ is a mean-zero Gaussian process independent of $(B_t)_{t\in\mathbb{R}_{\geqslant 0}}$, with covariance function $\mathbf{E}\xi_\alpha\xi_\beta = (\alpha+\beta)^{-1}$. This form is easily derived from (3.4) by setting

$$\xi_\beta := \int_{-\infty}^{0} e^{\beta s}\, dB_s \,.$$

CONNECTIONS. The derivation of (3.5) from the Mandelbrot-van Ness representation is presented in detail in Section 4.1 of this thesis.

In the course of his derivation, Muravlev obtained a related representation with a single expression that works for all $H \in (0, 1/2) \cup (1/2, 1)$. For arbitrary $\epsilon > 0$, the process

$$\overline{c}_H \int_0^\infty \left(\beta^{-1/2-H}(Z_t^\beta) - Z_0^\beta - e^{-\beta\epsilon_0} B_t\right) d\beta + \epsilon B_t,$$

where the constant

$$\epsilon_0 = \left(\frac{\epsilon}{\overline{c}_H \Gamma(1/2 - H)}\right)^{1/(H-1/2)},$$

specifies an H-fBm for $t \in [0, \infty)$.

The appeal of the Muravlev representation is that the function-valued process $(Z_t^\cdot)_{t\in\mathbb{R}_{\geqslant 0}}$ is a Markov process (see Section 4.2.2), and thus it provides an avenue through which some known theoretical tools for Markov processes can be applied to fBm. However, Harms and Stefanovits point out in [18, Rem. 3.6] that, contrary to a claim made by Muravlev, (3.5) cannot be described as a linear functional of an infinite-dimensional Markov process, because $(Z_t^{\cdot} - B_t)_{t\in\mathbb{R}_{\geqslant 0}}$ is not Markov. In [18, Thm. 3.5] they present an updated representation with more symmetric cases which *is* a linear functional of a Markov process. Up to a constant factor, it has the form

$$\begin{cases} \displaystyle\int_0^\infty \beta^{-1/2-H}(Z_t^\beta - Z_0^\beta)\, d\beta, & \text{if } H \in (0, 1/2), \\ \displaystyle\int_0^\infty \beta^{1/2-H}(Y_t^\beta - Y_0^\beta)\, d\beta, & \text{if } H \in (1/2, 1), \end{cases}$$

where, for each $\beta \in \mathbb{R}_{>0}$, the process $(Y_t^\beta)_{t\in\mathbb{R}_{\geqslant 0}}$ is related to $(Z_t^\beta)_{t\in\mathbb{R}_{\geqslant 0}}$ via the following stochastic differential equation:

$$dY_t^\beta = -\beta Y_t^\beta\, dt + Z_t^\beta\, dt\,.$$

APPLICATIONS. The Muravlev representation and its relatives have been used to obtain bounds on the expected value of an fBm at a (general) stopping time in terms of the mean of the stopping time [43, Thm. 2], to prove a conjectured inequality involving the maximum of an fBm [60, Thm 2.1], and to propose competitively-performing fBm approximation schemes [17].

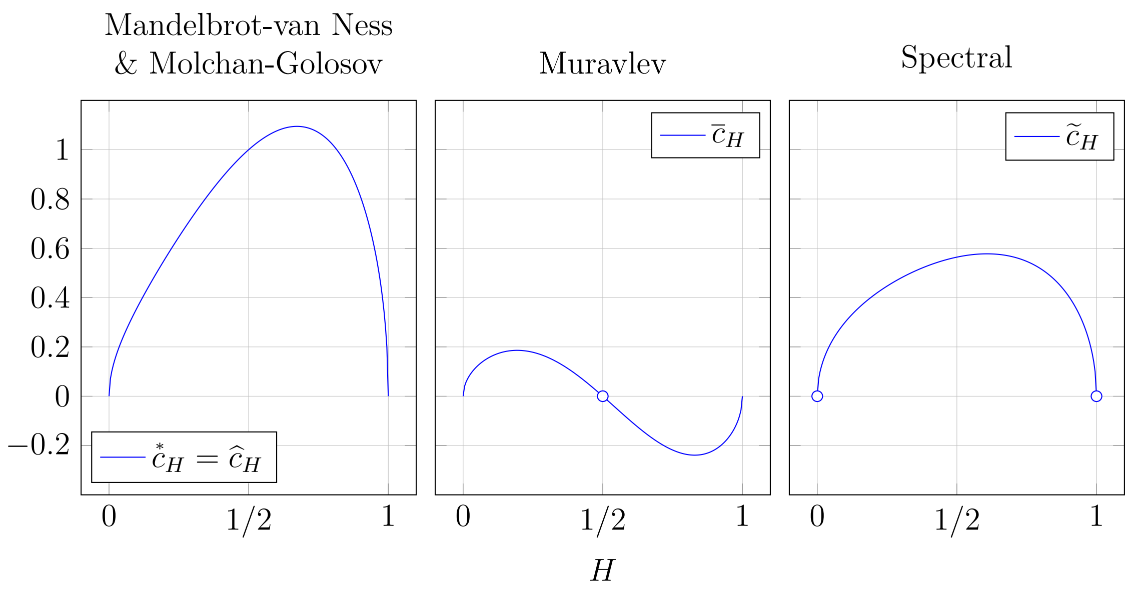

Figure 3.3: The constants in each of the four main representations described, plotted as functions of the Hurst parameter H. Excluding the three points indicated, values are defined on $H \in [0, 1]$.

3.1.2 Spectral domain

In the first of his two 1940 papers, Kolmogorov presented a spectral representation for fBm [24], albeit in a more general context and not under that name. The version presented here is less abstract.

Theorem 3.4 (spectral representation)**.** *Let* $H \in (0, 1/2) \cup (1/2, 1)$*, and* $(B_t)_{t\in\mathbb{R}}$ *be a standard Bm on the real line. If*

$$\widetilde{B}_t^H = \widetilde{c}_H \left(\int_{-\infty}^{0} \frac{1-\cos(st)}{|s|^{H+1/2}}\, dB_s + \int_0^\infty \frac{\sin(st)}{|s|^{H+1/2}}\, dB_s \right), \tag{3.6}$$

where the constant

$$\widetilde{c}_H = \left(2\int_0^\infty \frac{1-\cos s}{s^{2H+1}}\, ds \right)^{-\frac{1}{2}} = \left[-2\Gamma(-2H)\cos(\pi H) \right]^{-\frac{1}{2}},$$

then $(\widetilde{B}_t^H)_{t\in\mathbb{R}_{\geqslant 0}}$ *is an* H*-fBm.*

See [46, Prop. 2.3] for the proof. Several effectively equivalent variations exist, in particular some that define an fBm on the real line—see eg. [21, Thm. 3.6].

CONNECTIONS. The spectral representation can be related to the Mandelbrot-van Ness representation via Parseval's identity, see [21, Sec. 3.4] and [55, Sec. 7.2.2] for details.

As was the case for the Mandelbrot-van Ness representation, the (3.6) is one of a class of structurally similar representations. One such generalisation, analogous to (3.2), is noted in [55, Sec. 7.2.2].

In [10], the spectral representation is used to obtain a series representation of an H-fBm on $t \in [0,1]$ of the form

$$\sum_{n=1}^\infty \frac{1-\cos(x_n t)}{x_n} X_n + \sum_{n=1}^\infty \frac{\sin(y_n t)}{y_n} Y_n,$$

where $(x_n)_{n=1}^\infty$, $(y_n)_{n=1}^\infty$ are particular strictly increasing sequences of constants and $(X_n)_{n=1}^\infty$, $(Y_n)_{n=1}^\infty$ are independent sequences of independent, mean-zero normal random variables with particular variances dependent on n. A so-called Paley-Wiener expansion with a similar form is derived in [11, Cor. 8.2].

A second class of spectral-domain representations of fBm are those given by wavelet expansions (eg. [36, Thm. 2], [52, Thm. 8.2.7]), but the theory of wavelets is beyond the scope of this thesis.

3.2 Transformations

Transformation formulae for fractional Brownian motions are representations in which, for arbitrarily chosen Hurst parameters $H, K \in (0,1)$, an H-fBm is represented as a function of a K-fBm. Two of the previously introduced representations have been generalised to transformation formulae, stated below.

Both generalisations make use of stochastic integration with respect to an fBm. There are several approaches to defining such integrals, see [37, Ch. 1-2] for a comprehensive overview. The integrals that appear in Theorems 3.5 and 3.6 are *(fractional) Wiener integrals*, the construction of which is beyond the scope of this thesis. The reader is pointed to [20, Sec. 4] or the previous reference for details.

We now state the two transformation formulae. The first, a generalisation of the Mandelbrot-van Ness representation, was proved in [49, Thm. 1].

Theorem 3.5 (Mandelbrot-van Ness transformation)**.** *Let $H, K \in (0,1)$, and $(B_t^K)_{t\in\mathbb{R}}$ be a K-fBm. If*

$$\overset{*}{B}{}_t^{H,K} = \overset{*}{c}_{H,K} \int_{\mathbb{R}} \Big((t-s)_+^{H-K} - (-s)_+^{H-K} \Big)\, dB_s^K, \tag{3.7}$$

where the constant

$$\overset{*}{c}_{H,K} = \frac{1}{\Gamma(H-K+1)} \left(\frac{\Gamma(2H+1)\sin(\pi H)}{\Gamma(2K+1)\sin(\pi K)} \right)^{\frac{1}{2}},$$

then $(\overset{*}{B}{}_t^{H,K})_{t\in\mathbb{R}}$ is an H-fBm.

The second, an analogous generalisation of the Molchan-Golosov representation, was proved in [20, Thm. 5.1].

Theorem 3.6 (Molchan-Golosov transformation)**.** *Let $H, K \in (0,1)$, and $(B_t^K)_{t\in\mathbb{R}_{\geqslant 0}}$ be a K-fBm. If*

$$\widehat{B}_t^{H,K} = \widehat{c}_{H,K} \int_0^t (t-s)^{H-K} {}_2F_1\left(1-K-H, H-K, 1+H-K, \frac{s-t}{s}\right) dB_s^K, \tag{3.8}$$

where the constant

$$\widehat{c}_{H,K} = \frac{1}{\Gamma(H-K+1)} \left(\frac{2H\ \Gamma(H+1/2)\Gamma(3/2-H)\Gamma(2-2K)}{2K\ \Gamma(K+1/2)\Gamma(3/2-K)\Gamma(2-2H)} \right)^{\frac{1}{2}},$$

then $(\widehat{B}_t^{H,K})_{t\in\mathbb{R}_{\geqslant 0}}$ is an H-fBm.

Chapter 4

The Muravlev representation

Here, we investigate four aspects of the Muravlev representation of fractional Brownian motion (Theorem 3.3). They are (i) its derivation, (ii) the smoothness of the random field Z_t^β in β, (iii) the Markov property of the function-valued process $(Z_t^\cdot)_{t\in\mathbb{R}_{\geqslant 0}}$, and (iv) the emergence of long-range dependence.

4.1 Derivation

Muravlev [43] only provides a sketch of the derivation for his representation. Here we present it in more detail, drawing on a key integral form for the analytic continuation of the gamma function mentioned in [18, Rem. 3.6].

Lemma 4.1. *For $\tau \in \mathbb{R}_{>0}$ and $H \in (0, 1/2) \cup (1/2, 1)$ we have the following formulae.*

$$\tau^{H-1/2}\Gamma(1/2 - H) = \begin{cases} \displaystyle\int_0^\infty \beta^{-1/2-H} e^{-\tau\beta}\, d\beta, & \text{if } H \in (0, 1/2), \\ \displaystyle\int_0^\infty \beta^{-1/2-H} \left(e^{-\tau\beta} - 1\right) d\beta, & \text{if } H \in (1/2, 1). \end{cases} \tag{4.1}$$

Proof. We do each case separately.

For $H \in (0, 1/2)$, the integral on the right-hand side converges because the integrand is $O(\beta^{-1/2-H})$ as $\beta \searrow 0$ and $O(e^{-\tau\beta})$ as $\beta \to \infty$. The left-hand side arises via the substitution $u = \beta\tau$ and, since $1/2 - H > 0$, the standard integral definition of the gamma function. Note that this result can also be thought of as expressing the function $\tau \mapsto \tau^{H-1/2}$ as the Laplace transform of the function $\beta \mapsto \beta^{-1/2-H}/\Gamma(1/2 - H)$.

Now to $H \in (1/2, 1)$. The integral on the right-hand side converges because the integrand is $O(\beta^{1/2-H})$ as $\beta \searrow 0$ and $O(\beta^{-1/2-H})$ as $\beta \to \infty$. The integral definition of $\Gamma(x)$ does not converge for $x < 0$, but the definition can be extended via the identity $x\Gamma(x) = \Gamma(x + 1)$. In particular, for $x \in (-1, 0)$ one has

$$\begin{aligned} \Gamma(x) &= \frac{1}{x}\Gamma(x+1) = \frac{1}{x}\int_0^\infty u^x e^{-u}\, du \\ &= \frac{1}{x}\left(\Big[-u^x(e^{-u} - 1)\Big]_{u=0}^\infty + \int_0^\infty x u^{x-1}(e^{-u} - 1)\, du\right) = \int_0^\infty u^{x-1}(e^{-u} - 1)\, du, \end{aligned}$$

using integration by parts. Each of these integrals converges, as per the comments above. Again, substituting $u = \beta\tau$ into the integral on the right-hand side of (4.1), we see that

$$\int_0^\infty \beta^{-1/2-H}\left(e^{-\beta\tau}-1\right)d\beta = \tau^{H-1/2}\int_0^\infty u^{(1/2-H)-1}\left(e^{-u}-1\right)du$$
$$= \tau^{H-1/2}\Gamma(1/2-H). \qquad \square$$

We can now proceed to the derivation of the Muravlev representation.

Proof of Theorem 3.3. Start with Theorem 3.1, the Mandelbrot-van Ness representation. For $t \in \mathbb{R}_{\geqslant 0}$,

$$\begin{aligned}
\overset{*}{B}{}_t^H &= \overset{*}{c}_H \int_{\mathbb{R}} \left((t-s)_+^{H-1/2} - (-s)_+^{H-1/2}\right) dB_s \\
&= \overset{*}{c}_H \int_{-\infty}^0 \left((t-s)^{H-1/2} - (-s)^{H-1/2}\right) dB_s + \overset{*}{c}_H \int_0^t (t-s)^{H-1/2}\, dB_s \\
&= \begin{cases}
\overline{c}_H \displaystyle\int_{-\infty}^0 \left[\int_0^\infty \beta^{-1/2-H}(e^{-\beta(t-s)} - e^{\beta s})\, d\beta\right] dB_s \\
\qquad + \overline{c}_H \displaystyle\int_0^t \left[\int_0^\infty \beta^{-1/2-H} e^{-\beta(t-s)}\, d\beta\right] dB_s, & \text{if } H \in (0, 1/2), \\
\overline{c}_H \displaystyle\int_{-\infty}^0 \left[\int_0^\infty \beta^{-1/2-H}(e^{-\beta(t-s)} - e^{\beta s})\, d\beta\right] dB_s \\
\qquad + \overline{c}_H \displaystyle\int_0^t \left[\int_0^\infty \beta^{-1/2-H} \left(e^{-\beta(t-s)} - 1\right) d\beta\right] dB_s, & \text{if } H \in (1/2, 1).
\end{cases}
\end{aligned}$$

The final equality follows from Lemma 4.1 and the identity $\overset{*}{c}_H = \overline{c}_H \Gamma(1/2 - H)$, which holds because

$$B(1/2 + H, 1/2 - H) = \frac{\Gamma(1/2 + H)\Gamma(1/2 - H)}{\Gamma(1)},$$

and $\Gamma(1) = 1$. Each of the integrals in the final expression converges, as per comments in the proof of Lemma 4.1. Using a stochastic Fubini theorem (see [29, Thm. 5.15]) to interchange the order of integration and defining,

$$Z_t^\beta := \int_{-\infty}^t e^{-\beta(t-s)}\, dB_s, \tag{4.2}$$

we get

$$\overline{B}_t^H = \begin{cases}
\overline{c}_H \displaystyle\int_0^\infty \beta^{-1/2-H}(Z_t^\beta - Z_0^\beta)\, d\beta, & \text{if } H \in (0, 1/2)\,, \\
\overline{c}_H \displaystyle\int_0^\infty \beta^{-1/2-H}(Z_t^\beta - Z_0^\beta - B_t)\, d\beta, & \text{if } H \in (1/2, 1)\,,
\end{cases}$$

which is the Muravlev representation. $\square$

4.2 The random field Z_t^β

The core stochastic object appearing in the Muravlev representation is the Gaussian random field $Z_t^\beta = (Z_t^\beta)_{t\in\mathbb{R}_{\geqslant 0}, \beta\in\mathbb{R}_{>0}}$. A portion of a sample surface is shown in Figure 4.1. Here we prove that, for each $t \in \mathbb{R}_{\geqslant 0}$, sample paths of the one-dimensional slice $(Z_t^\beta)_{\beta\in\mathbb{R}_{>0}}$ are smooth. We then show that, when viewed as an infinite-dimensional Ornstein-Uhlenbeck process, $(Z_t^{\cdot})_{t\in\mathbb{R}_{\geqslant 0}}$ is Markov, and compute its transition probabilities.

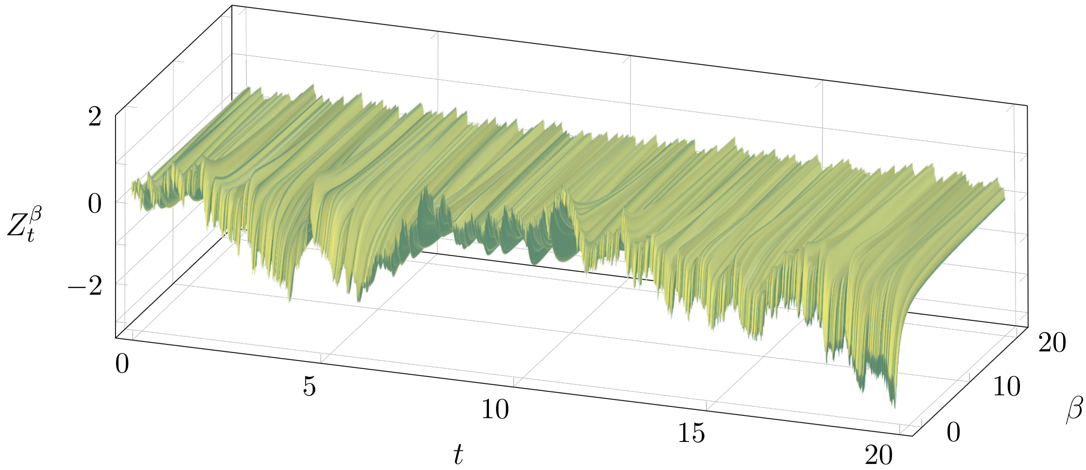

Figure 4.1: The random field Z_t^β sampled on the grid: $t = 0.01(k-1)$ for $k \in \mathbb{N}_{\leqslant 2001}$, and $\beta = 0.05m$ for $m \in \mathbb{N}_{\leqslant 400}$. The vertical cross-sections of the surface parallel to the t axis are Ornstein-Uhlenbeck processes, and hence rough. The vertical cross-sections parallel to the β axis are smooth Gaussian processes with covariance $\mathbf{E} Z_t^\alpha Z_t^\beta = (\alpha+\beta)^{-1}$. Variance of the random field approaches infinity as $\beta \searrow 0$ and zero as $\beta \to \infty$. Note that the process was started in stationarity as per (4.2), though in this particular sample, it is difficult to distinguish from an initial value of $Z_0^\cdot \equiv 0$. The code used to generate the sample can be found in the appendix.

4.2.1 Smoothness in β

We start with a prerequisite lemma, adapted from [13, Thm. 2.27].

Lemma 4.2 (differentiation under integral)**.** *For $-\infty \leqslant a < b \leqslant \infty$, let*

$$f : \mathrm{S} \times (a,b) \to \mathbb{R}$$

be a function such that $f(\cdot, x) : \mathrm{S} \to \mathbb{R}$ is integrable and measurable for all $x \in (a,b)$. If $\partial_x f$ exists and further there exists an integrable function $g : \mathrm{S} \to \mathbb{R}$ such that

$$|\partial_x f(s,x)| \leqslant g(s), \qquad \text{for all } x \in (a,b),\ s \in \mathrm{S},$$

then $\int_{\mathrm{S}} f(s,x)\,ds$ is differentiable in x and

$$\partial_x \int_{\mathrm{S}} f(s,x)\,ds = \int_{\mathrm{S}} \partial_x f(s,x)\,ds\,.$$

Proof. Fix $x \in (a,b)$. For any real sequence $(h_n)_{n=1}^\infty$ such that $h_n \to 0$ as $n \to \infty$, we have $\partial_x f(s,x) = \lim_{n\to\infty} f_n(s)$, where

$$f_n(s) := \frac{f(s, x+h_n) - f(s,x)}{h_n}.$$

The functions f_n are compositions of measurable functions so are themselves measurable. Additionally, $f_n(s) \to \partial_x f(s,x)$ pointwise for all $s \in \mathrm{S}$ and the inequality

$$|f_n(s)| \leqslant \sup_{y\in(a,b)} \left|\partial_y f(s,y)\right| \leqslant g(s)$$

holds by assumption. Thus, applying the dominated convergence theorem (DCT), we see that $\partial_x f(s,x)$ is integrable in s, so $\partial_x \int_{\mathrm{S}} f(s,x)\,ds$ exists and is given by

$$\begin{aligned}\partial_x \int_{\mathrm{S}} f(s,x)\,ds &= \lim_{n\to\infty} \frac{1}{h_n}\left[\int_{\mathrm{S}} f(s,x+h_n)\,ds - \int_{\mathrm{S}} f(s,x)\,ds\right] \\ &= \lim_{n\to\infty} \int_{\mathrm{S}} f_n(s)\,ds \overset{\mathsf{DCT}}{=} \int_{\mathrm{S}} \partial_x f(s,x)\,ds\,. \qquad \square\end{aligned}$$

Theorem 4.1 (smoothness of Z_t^β in β)**.** *For any $k \in \mathbb{N}$ and any fixed $t \in \mathbb{R}_{\geqslant 0}$, the derivative $\partial_\beta^k Z_t^\beta$ exists and is continuous in β.*

Proof. By Theorem 2.3 (Itô's formula),

$$d(e^{\beta\cdot}B_\cdot)_t = \beta e^{\beta t} B_t\,ds + e^{\beta t}\,dB_t\,.$$

So, multiplying the corresponding integral equation with terminals $\int_{-\infty}^t$ by $e^{-\beta t}$, we see that Z_t^β can be rewritten as a Lebesgue integral:

$$\begin{aligned} Z_t^\beta &= \int_{-\infty}^t e^{\beta(s-t)}\,dB_s \\ &= \left[e^{\beta(s-t)}B_s\right]_{s=-\infty}^t - \int_{-\infty}^t \beta e^{\beta(s-t)}B_s\,ds \\ &= B_t - \int_{-\infty}^t \beta e^{\beta(s-t)}B_s\,ds\,. \end{aligned}$$

In the last equality, we used the law of the iterated logarithm (LIL) for Bm (see eg. [42, Thm. 5.1]), which implies that $B_s = O(|s|)$ almost surely as $|s| \to \infty$.

Let $k \in \mathbb{N}$ be arbitrary. The above integrand is smooth in β so $\partial_\beta^k \beta e^{\beta(s-t)}B_s$ exists. Since B_t is almost surely continuous and $|B_t/t| \xrightarrow{a.s.} 0$ as $|t| \to \infty$ (a consequence of the LIL), there exists a random time $T_k \in (-\infty, 0)$ such that for all $\beta \in \mathbb{R}_{>0}$,

$$g_k(s) := \begin{cases} \partial_\beta^k \beta e^{\beta(s-t)}|s|, & \text{if } s \in (-\infty, T_k), \\ \partial_\beta^k \beta e^{\beta(s-t)}\left(\sup_{u\in[T_k,t]} |B_u|\right), & \text{if } s \in [T_k, t], \end{cases}$$

is an integrable upper bound for $\left|\partial_\beta^k \beta e^{\beta(s-t)}B_s\right|$ on $s \in (-\infty, t]$. Further, as a function of s, $\partial_\beta^{k-1} \beta e^{\beta(s-t)}B_s$ is integrable and measurable a.s. on $(\infty, t]$. So the conditions of Lemma 4.2 are satisfied for all $k \in \mathbb{N}$ and, if $n \in \mathbb{N}$, we have

$$\begin{aligned} \partial_\beta^n Z_t^\beta &= \partial_\beta^n B_t - \partial_\beta^n \int_{-\infty}^t \beta e^{\beta(s-t)}B_s\,ds \\ &= -\underbrace{\partial_\beta \ldots \partial_\beta}_{n \text{ derivatives}} \int_{-\infty}^t \beta e^{\beta(s-t)}B_s\,ds \\ &= -\int_{-\infty}^t \partial_\beta^n \beta e^{\beta(s-t)}B_s\,ds\,. \end{aligned}$$

For the last equality, we repeatedly used Lemma 4.2 and dominating function g_{k+1} to move the k-th ($k \in \mathbb{N}_{\leqslant n}$) partial derivative under the integral. Thus $\partial_\beta^k Z_t^\beta$ exists for all $k \in \mathbb{N}$ and, since $\partial_\beta^{k+1} Z_t^\beta$ also exists, $\partial_\beta^k Z_t^\beta$ is continuous in β. $\square$

4.2.2 As a Markov process

Multivariate Ornstein-Uhlenbeck process

The *matrix exponential* e^A for a matrix $A \in \mathbb{R}^{m\times m}$ is defined (as per [54]) by

$$e^A := \sum_{n=0}^{\infty} \frac{A^n}{n!}. \tag{4.3}$$

In this thesis, we will work with vectors as column vectors, and use $\cdot'$ to denote the transpose of a vector or matrix. If $A = \mathsf{diag}((a_1, \dots, a_m)')$, the $m \times m$ diagonal matrix with elements of the column vector $(a_1, \dots, a_m)'$ along the diagonal, then (4.3) implies that $e^A = \mathsf{diag}((e^{a_1}, \dots, e^{a_m})')$. This is the only case we will encounter.

For arbitrary $m \in \mathbb{N}$, let $\boldsymbol{\beta} = (\beta_1, \dots, \beta_m)' \in \mathbb{R}^m_{>0}$, and $\boldsymbol{Z}_t^{\boldsymbol{\beta}} = (Z_t^{\beta_1}, \dots, Z_t^{\beta_m})'$. Following [34], we can describe $(\boldsymbol{Z}_t^{\boldsymbol{\beta}})_{t\in\mathbb{R}_{\geqslant 0}}$ as a multivariate Ornstein-Uhlenbeck process with the following integral representation:

$$\begin{aligned}\boldsymbol{Z}_t^{\boldsymbol{\beta}} &= e^{-\mathsf{diag}(\boldsymbol{\beta})t}\boldsymbol{Z}_0^{\boldsymbol{\beta}} + \int_0^t e^{-\mathsf{diag}(\boldsymbol{\beta})(t-u)}\mathbf{1}_m\, dB_u \\ &= \int_{-\infty}^t e^{-\mathsf{diag}(\boldsymbol{\beta})(t-u)}\mathbf{1}_m\, dB_u\,.\end{aligned}$$

The vector integrals are evaluated element-wise. Generalising the univariate case, $(\boldsymbol{Z}_t^{\boldsymbol{\beta}})_{t\in\mathbb{R}_{\geqslant 0}}$ can also be shown to be the unique strong solution of the following multivariate SDE:

$$d\boldsymbol{Z}_t^{\boldsymbol{\beta}} = -\mathsf{diag}(\boldsymbol{\beta})\boldsymbol{Z}_t^{\boldsymbol{\beta}}\, dt + \mathbf{1}_m\, dB_t, \quad \text{for } t \in \mathbb{R}_{>0},\ \boldsymbol{Z}_0^{\boldsymbol{\beta}} = \int_{-\infty}^0 e^{-\mathsf{diag}(\boldsymbol{\beta})(t-u)}\mathbf{1}_m\, dB_u\,.$$

The transition densities for $(\boldsymbol{Z}_t^{\boldsymbol{\beta}})_{t\in\mathbb{R}_{\geqslant 0}}$ will be required shortly, so we compute them here. Fix arbitrary $s, t \in \mathbb{R}_{\geqslant 0}$ such that $s < t$. Then

$$\begin{aligned}\boldsymbol{Z}_t^{\boldsymbol{\beta}} &= \int_{-\infty}^t e^{-\mathsf{diag}(\boldsymbol{\beta})(t-u)}\mathbf{1}_m\, dB_u \\ &= e^{-\mathsf{diag}(\boldsymbol{\beta})(t-s)}\int_{-\infty}^s e^{-\mathsf{diag}(\boldsymbol{\beta})(s-u)}\mathbf{1}_m\, dB_u + \int_s^t e^{-\mathsf{diag}(\boldsymbol{\beta})(t-u)}\mathbf{1}_m\, dB_u \\ &= e^{-\mathsf{diag}(\boldsymbol{\beta})(t-s)}\boldsymbol{Z}_s^{\boldsymbol{\beta}} + \int_s^t e^{-\mathsf{diag}(\boldsymbol{\beta})(t-u)}\mathbf{1}_m\, dB_u\,.\end{aligned} \tag{4.4}$$

The second term is a vector of Itô integrals with a shared Bm driver $(B_u)_{u\in[s,t]}$, so can be defined as a limit of a sequence of linear transformations of the increments of B_u. Each element in the sequence, being a linear transformation of a vector of independent Bm increments, is multivariate Gaussian, and so the limiting vector of integrals will also be multivariate Gaussian. As such, the conditional distribution of $\boldsymbol{Z}_t^{\boldsymbol{\beta}}|\boldsymbol{Z}_s^{\boldsymbol{\beta}}$ is fully specified by its mean vector and covariance matrix. Using (4.4), the mean is given by

$$\begin{aligned}\boldsymbol{\mu}_{t|s,\boldsymbol{Z}_s^{\boldsymbol{\beta}}} := \mathbf{E}\left[\boldsymbol{Z}_t^{\boldsymbol{\beta}}|\boldsymbol{Z}_s^{\boldsymbol{\beta}}\right] &= \mathbf{E}\left[e^{-\mathsf{diag}(\boldsymbol{\beta})(t-s)}\boldsymbol{Z}_s^{\boldsymbol{\beta}}|\boldsymbol{Z}_s^{\boldsymbol{\beta}}\right] + \mathbf{E}\left[\int_s^t e^{-\mathsf{diag}(\boldsymbol{\beta})(t-u)}\mathbf{1}_m\, dB_u\,|\boldsymbol{Z}_s^{\boldsymbol{\beta}}\right] \\ &= e^{-\mathsf{diag}(\boldsymbol{\beta})(t-s)}\boldsymbol{Z}_s^{\boldsymbol{\beta}} + \mathbf{0}_m = e^{-\mathsf{diag}(\boldsymbol{\beta})(t-s)}\boldsymbol{Z}_s^{\boldsymbol{\beta}},\end{aligned}$$

and the covariance matrix by

$$\begin{aligned}
\boldsymbol{\Sigma}_{t|s,\boldsymbol{Z}_s^\beta} &:= \mathbf{E}\left[\left(\boldsymbol{Z}_t^\beta - \mathbf{E}\left[\boldsymbol{Z}_t^\beta|\boldsymbol{Z}_s^\beta\right]\right)\left(\boldsymbol{Z}_t^\beta - \mathbf{E}\left[\boldsymbol{Z}_t^\beta|\boldsymbol{Z}_s^\beta\right]\right)'|\boldsymbol{Z}_s^\beta\right] \\
&= \mathbf{E}\left[\left(\int_s^t e^{-\mathsf{diag}(\beta)(t-u)}\mathbf{1}_m\,dB_u\right)\left(\int_s^t e^{-\mathsf{diag}(\beta)(t-u)}\mathbf{1}_m\,dB_u\right)'|\boldsymbol{Z}_s^\beta\right] \\
&= \left[\mathbf{E}\left[\left(\int_s^t e^{-\beta_i(t-u)}\,dB_u\right)\left(\int_s^t e^{-\beta_j(t-u)}\,dB_u\right)\right]\right]_{i,j=1}^m \\
&= \left[\int_s^t e^{-\beta_i(t-u)}e^{-\beta_j(t-u)}\,du\right]_{i,j=1}^m \\
&= \left[\frac{1-e^{-(\beta_i+\beta_j)(t-s)}}{\beta_i+\beta_j}\right]_{i,j=1}^m .
\end{aligned}$$

In the second-last equality, we used the standard expression for the covariance of Itô integrals, which can be derived from the Itô isometry using the polarisation identity. Thus, $\boldsymbol{Z}_t^\beta|\boldsymbol{Z}_s^\beta \sim \mathrm{MVN}(\boldsymbol{\mu}_{t|s,\boldsymbol{Z}_s^\beta}, \boldsymbol{\Sigma}_{t|s,\boldsymbol{Z}_s^\beta})$ and has the corresponding transition density:

$$f_{t|s,\boldsymbol{Z}_s^\beta}(\boldsymbol{z}) = \frac{1}{(2\pi)^{m/2}\sqrt{\det(\boldsymbol{\Sigma}_{t|s,\boldsymbol{Z}_s^\beta})}}\exp\left\{-\frac{1}{2}(\boldsymbol{z}-\boldsymbol{\mu}_{t|s,\boldsymbol{Z}_s^\beta})'\boldsymbol{\Sigma}_{t|s,\boldsymbol{Z}_s^\beta}^{-1}(\boldsymbol{z}-\boldsymbol{\mu}_{t|s,\boldsymbol{Z}_s^\beta})\right\}. \tag{4.5}$$

In the limiting case $s = t$, set $f_{s|s,\boldsymbol{Z}_s^\beta}(\boldsymbol{z}) := \delta_{\boldsymbol{Z}_s^\beta}(\boldsymbol{z})$, where $\delta_{\boldsymbol{Z}_s^\beta}$ is the m-dimensional Dirac delta function positioned at $\boldsymbol{Z}_s^\beta$.

Formalisation of $(Z_t^\cdot)_{t\in\mathbb{R}_{\geqslant 0}}$ as a Markov process

Denote by Ω the underlying sample space, equipped with the σ-algebra $\mathcal{F}$ generated by the standard Bm $(B_t)_{t\in\mathbb{R}}$ on the real line, and the filtration $\mathcal{F}_t = \sigma((B_s)_{s\leqslant t})$.

Consider the process $Z = (Z_t^\cdot)_{t\in\mathbb{R}_{\geqslant 0}}$ where, for each $t \in \mathbb{R}_{\geqslant 0}$, Z_t is the function $Z_t^\cdot : \mathbb{R}_{>0} \times \Omega \to \mathbb{R}$ mapping $(\beta,\omega) \mapsto Z_t^\beta(\omega)$. Theorem 4.1 implies Z_t^β is continuous in β, so for fixed ω, $(Z_t^\cdot)_{t\in\mathbb{R}_{\geqslant 0}}$ takes values in $C(0,\infty)$, the set of continuous functions on $(0,\infty)$. The notation $Z_t(\beta) := Z_t^\beta$ will be used to emphasise that $Z_t^\cdot$ is a function of β, with the dependence on ω implicit.

Let $\mathcal{E}$ be the σ-algebra on $C(0,\infty)$ generated by so-called *cylindrical* subsets which have the form

$$\bigcap_{j=1}^m \{h \in C(0,\infty) : h(\beta_j) \in E_j\}, \quad \text{where } \beta_j \in \mathbb{R}_{>0}, E_j \in \mathscr{B}(\mathbb{R})\ \forall\ j \in \mathbb{N}_{\leqslant m}, \tag{4.6}$$

and $m \in \mathbb{N}$ can depend on the subset. The vector $\boldsymbol{\beta} = (\beta_1,\ldots,\beta_m)' \in \mathbb{R}_{>0}^m$ we will call the *grid* of the cylinder.

Following Definition 2.5, we wish to construct a family of probability measures $\{P_{s,g} \mid s \in \mathbb{R}_{\geqslant 0}, g \in C(0,\infty)\}$ on $\mathcal{F}$ such that $(Z,\mathcal{F}_t,P_{s,g})$ is a Markov process. For brevity, we will restrict ourselves to constructing such measures $P_{s,g}$ only on sets of the form $\{Z_t^\cdot \in E\}$ for some $E \in \mathcal{E}$, and adopt the shorthand $P_{t|s,g}(E) := P_{s,g}(\{X_t^\cdot \in E\})$.

As a starting point, we will explicitly define a narrower class of probability measures $P^{\boldsymbol\beta}_{t|s,g}$ on cylinders with the grid $\boldsymbol\beta$.

Fix arbitrary $s \in \mathbb{R}_{\geqslant 0}$, $g \in C(0,\infty)$, and let E be a cylinder with grid $\boldsymbol\beta$. Using the multivariate Ornstein-Uhlenbeck framework, the probability $P^{\boldsymbol\beta}_{t|s,g}(E)$ can be defined as follows:

$$\begin{aligned} P^{\boldsymbol\beta}_{t|s,g}(E) &\overset{(4.6)}{=} P^{\boldsymbol\beta}_{t|s,g}\left(\bigcap_{j=1}^{m}\{h \in C(0,\infty) : h(\beta_j) \in E_j\}\right) \\ &:= \mathbf{P}\left(\left\{\boldsymbol{Z}^{\boldsymbol\beta}_t \in E_1 \times \cdots \times E_m \mid \boldsymbol{Z}^{\boldsymbol\beta}_s = g^{\boldsymbol\beta}\right\}\right) \\ &= \int_{E_1\times\cdots\times E_m} f_{t|s,g^{\boldsymbol\beta}}(\boldsymbol{z})\, d\boldsymbol{z} \end{aligned} \tag{4.7}$$

where $g^{\boldsymbol\beta} = (g(\beta_1), \ldots, g(\beta_m))'$ and $f_{t|s,g^{\boldsymbol\beta}}$ is the transition density for the finite-dimensional multivariate Ornstein-Uhlenbeck process described in Equation 4.5.

Having defined the probability measure $P^{\boldsymbol\beta}_{t|s,g}$ on the finite-dimensional cylinders of the form (4.6), we can extend it to all sets $E \in \mathcal{E}$ using the Kolmogorov extension theorem (KET). The following statement is modelled on that given in [47, Thm.2.1.5].

Theorem 4.2 (Kolmogorov extension theorem)**.** *Let* B *be an arbitrary index set, and* $\{P^{\boldsymbol b} \mid \boldsymbol{b} = (b_1, \ldots, b_m)' \in \mathrm{B}^m, m \in \mathbb{N}\}$ *be a family of probability measures on* $\mathbb{R}^m$ *(m depends on the measure) satisfying the following two consistency conditions:*

i. For all sets $E_i \in \mathscr{B}(\mathbb{R})$, $i \in \mathbb{N}_{\leqslant m}$, *indices* $\boldsymbol{b} \in \mathrm{B}^m$, $m \in \mathbb{N}$, *and permutations* π *of* $\{1, \ldots, m\}$,

$$P^{(b_1,\ldots,b_m)'}(E_1 \times \cdots \times E_m) = P^{(b_{\pi(1)},\ldots,b_{\pi(m)})'}(E_{\pi(1)} \times \cdots \times E_{\pi(m)}).$$

ii. For all sets $E_i \in \mathscr{B}(\mathbb{R})$, $i \in \mathbb{N}_{\leqslant m}$, *and indices* $\boldsymbol{b} \in \mathrm{B}^{m+k}$, $m, k \in \mathbb{N}$,

$$P^{(b_1,\ldots,b_m)'}(E_1 \times \cdots \times E_m) = P^{\boldsymbol b}\left(E_1 \times \cdots \times E_m \times \mathbb{R}^k\right).$$

Then there exists a probability space $(\Omega, \mathcal{F}, P)$ *and a stochastic process* $X : \mathrm{B} \times \Omega \to \mathbb{R}$ *such that for all indices* $\boldsymbol{b} = (b_1, \ldots, b_m)' \in \mathrm{B}^m$ *and sets* $E_i \in \mathscr{B}(\mathbb{R})$, $i \in \mathbb{N}_{\leqslant m}$,

$$P(X_{b_1} \in E_1, \ldots, X_{b_m} \in E_n) = P^{\boldsymbol\beta}(E_1 \times \cdots \times E_m).$$

For arbitrary fixed $s, t \in \mathbb{R}_{\geqslant 0}$, $g \in C(0,\infty)$, the set $\{P^{\boldsymbol\beta}_{t|s,g} : \boldsymbol\beta \in \mathbb{R}^m, m \in \mathbb{N}\}$ is a family of probability measures on $\mathbb{R}^m$. From the explicit formula (4.7), it is clear that the family satisfies condition (i) because of the invariance of the integral and density under permutations of $((\beta_i, E_i))_{i=1}^m$, and (ii) because integrating the density over $\mathbb{R}$ with respect to particular β_j simply returns the marginal density for the remaining elements of $\boldsymbol\beta$. Thus, by the Kolmogorov extension theorem, there exists a probability measure $P_{t|s,g}$ and process—namely $(Z_t^\beta)_{\beta\in\mathbb{R}_{>0}}$—with finite dimensional distributions specified by $P^{\boldsymbol\beta}_{t|s,g}$, for each $\boldsymbol\beta \in \mathbb{R}^m$.

We can now prove the following.

Theorem 4.3. $(Z, \mathcal{F}_t, P_{s,g})$ *is a Markov process.*

The proof requires that the four conditions in Definition 2.5 are satisfied. Conditions **M**1-**M**3 are satisfied, but quite technical. In the interest of readability, only the proof of the Markov property **M**4 is included in full, while brief comments are made about **M**1-**M**3.

M1 The random variable $Z_t : \Omega \to \mathbb{C}(0,\infty)$ is defined as a measurable function of $(B_s)_{s\leqslant t}$, which is $\mathcal{F}_t$-measurable by the definition of $\mathcal{F}_t$.

M2 Using the explicit form (4.7) for $P^{\boldsymbol{\beta}}_{t|s,g}(E)$ on cylinders E with grid $\boldsymbol{\beta}$, the function for general E can be constructed by taking limits and compositions of measurable functions.

M3 The event $\{Z_s^{\cdot} \in C(0,\infty) \setminus g\}$ is a subset of the event $E := \{Z_s^1 \in \mathbb{R} \setminus \{g(1)\}\}$, and the probability $P_{s,g}(E) = 0$ because it is defined as an integral over a Dirac delta function on a domain which excludes the point at which the integrand has mass.

Proof of the Markov property (**M**4)*.* Take arbitrary $g \in C(0,\infty)$, set $E \in \mathcal{E}$, and times $r, s, t \in \mathbb{R}_{\geqslant 0}$ such that $r \leqslant s \leqslant t$. Since

$$P_{s,Z_s^{\cdot}}(\{Z_t^{\cdot} \in E\}) = P_{r,g}(\{Z_t^{\cdot} \in E | Z_s\}),$$

the condition **M**4 that

$$P_{r,g}(\{Z_t^{\cdot} \in E | \mathcal{F}_s\}) = P_{s,Z_s^{\cdot}}(\{Z_t^{\cdot} \in E\}),$$

is equivalent to the condition that $Z_t^{\cdot} | \mathcal{F}_s \overset{d}{=} Z_t^{\cdot} | Z_s^{\cdot}$ under all probability measures $P_{r,g}$.

We note that the cylinders form a π-system, and recall that probability measures that agree on a π-system will agree on the σ-algebra generated by that π-system. Thus it is sufficient to show that $P_{r,g}(\{Z_t^{\cdot} \in E|\mathcal{F}_s\}) = P_{r,g}(\{Z_t^{\cdot} \in E|Z_s^{\cdot}\})$ for all cylinders E. On such cylinders with (arbitrary) grid $\boldsymbol{\beta}$, this is equivalent to showing that $\boldsymbol{Z}_t^{\boldsymbol{\beta}} | \mathcal{F}_s \overset{d}{=} \boldsymbol{Z}_t^{\boldsymbol{\beta}} | \boldsymbol{Z}_s^{\boldsymbol{\beta}}$.

This can be shown expediently using characteristic functions together with (4.4).

$$\begin{aligned}
\mathbf{E}\left[e^{i\boldsymbol{x}'\boldsymbol{Z}_t^{\boldsymbol{\beta}}} \middle| \mathcal{F}_s\right] &= \mathbf{E}\left[\exp\left\{i\boldsymbol{x}'\left(e^{-\mathsf{diag}(\boldsymbol{\beta})(t-s)}\boldsymbol{Z}_s^{\boldsymbol{\beta}} + \int_s^t e^{-\mathsf{diag}(\boldsymbol{\beta})(t-u)}\mathbf{1}_m\, dB_u\right)\right\} \middle| \mathcal{F}_s\right] \\
&= \exp\left\{i\boldsymbol{x}'\left(e^{-\mathsf{diag}(\boldsymbol{\beta})(t-s)}\boldsymbol{Z}_s^{\boldsymbol{\beta}}\right)\right\}\mathbf{E}\left[\exp\left\{i\boldsymbol{x}'\left(\int_s^t e^{-\mathsf{diag}(\boldsymbol{\beta})(t-u)}\mathbf{1}_m\, dB_u\right)\right\} \middle| \mathcal{F}_s\right] \\
&= \exp\left\{i\boldsymbol{x}'\left(e^{-\mathsf{diag}(\boldsymbol{\beta})(t-s)}\boldsymbol{Z}_s^{\boldsymbol{\beta}}\right)\right\}\mathbf{E}\left[\exp\left\{i\boldsymbol{x}'\left(\int_s^t e^{-\mathsf{diag}(\boldsymbol{\beta})(t-u)}\mathbf{1}_m\, dB_u\right)\right\} \middle| \boldsymbol{Z}_s^{\boldsymbol{\beta}}\right] \\
&= \mathbf{E}\left[\exp\left\{i\boldsymbol{x}'\left(e^{-\mathsf{diag}(\boldsymbol{\beta})(t-s)}\boldsymbol{Z}_s^{\boldsymbol{\beta}} + \int_s^t e^{-\mathsf{diag}(\boldsymbol{\beta})(t-u)}\mathbf{1}_m\, dB_u\right)\right\} \middle| \boldsymbol{Z}_s^{\boldsymbol{\beta}}\right] \\
&= \mathbf{E}\left[e^{i\boldsymbol{x}'\boldsymbol{Z}_t^{\boldsymbol{\beta}}} \middle| \boldsymbol{Z}_s^{\boldsymbol{\beta}}\right].
\end{aligned}$$

For the third equality, we used the fact that the random variable in the expectation is independent of both $\mathcal{F}_s$ and $\boldsymbol{Z}_s^{\boldsymbol{\beta}}$. Characteristic functions completely specify their corresponding distributions, so $\boldsymbol{Z}_t^{\boldsymbol{\beta}} | \mathcal{F}_s \overset{d}{=} \boldsymbol{Z}_t^{\boldsymbol{\beta}} | \boldsymbol{Z}_s^{\boldsymbol{\beta}}$, and hence the probability $P_{r,g}(\{Z_t^{\cdot} \in E|\mathcal{F}_s\}) = P_{s,Z_s^{\cdot}}(\{Z_t^{\cdot} \in E\})$ for all $E \in \mathcal{E}$. □

4.3 Long-range dependence

For each $\beta \in \mathbb{R}_{>0}$, the Ornstein-Uhlenbeck process $(Z_t^\beta)_{t\in\mathbb{R}_{\geqslant 0}}$ is short-range dependent. How does long-range dependence arise in $\overline{B}_t^H$, a weighted integral over short-range dependent processes?

In this section this phenomenon is investigated by looking at the presence of long-range dependence in the integrand(s) of $\overline{B}_t^H$ for fixed $\beta \in \mathbb{R}_{>0}$, and in the limits as $\beta \searrow 0$ and $\beta \to \infty$. As a starting point, we restrict our analysis to the random field Z_t^β. For this we will need two useful facts.

First, let us compute the covariance function of the random field Z_t^β. For parameters $\alpha, \beta \in \mathbb{R}_{>0}$ and $s, t \in \mathbb{R}_{\geqslant 0}$ such that $s \leqslant t$, the covariance of Z_s^α with Z_t^β is given by

$$\begin{aligned}
\mathbf{E} Z_s^\alpha Z_t^\beta &= \mathbf{E}\left[\int_{-\infty}^s e^{-\alpha(s-u)}\,dB_u \int_{-\infty}^t e^{-\beta(t-u)}\,dB_u\right] \\
&= e^{-\alpha s-\beta t}\mathbf{E}\left[\int_{-\infty}^s e^{\alpha u}\,dB_u \left(\int_{-\infty}^s e^{\beta u}\,dB_u + \int_s^t e^{\beta u}\,dB_u\right)\right] \\
&= e^{-\alpha s-\beta t}\mathbf{E}\left[\int_{-\infty}^s e^{\alpha u}\,dB_u \int_{-\infty}^s e^{\beta u}\,dB_u\right] \\
&= e^{-\alpha s-\beta t}\int_{-\infty}^s e^{(\alpha+\beta)u}\,du = \frac{1}{\alpha+\beta}e^{-\beta|t-s|}.
\end{aligned} \tag{4.8}$$

Second, we will require the value of a constant appearing in a mean value theorem-type formula for the function $x \mapsto e^{-\beta x}$. Specifically, for all $x \in \mathbb{R}$,

$$\frac{e^{-\beta x} - e^{-\beta(x-1)}}{x-(x-1)} = -\beta e^{-\beta(x-\theta_\beta)} \implies \theta_\beta = \frac{1}{\beta}\left[\log(e^\beta - 1) - \log(\beta)\right]. \tag{4.9}$$

Note that θ_β is independent of x, strictly increasing as a function of β and takes values in the interval $[0,1]$.

Now, using the initial equation in (4.9) three times, the autocovariance of the increment process $(Z_n^\beta - Z_{n-1}^\beta)_{n\in\mathbb{N}}$ can be obtained:

$$\begin{aligned}
\gamma_{Z^\beta}(n) &= \mathbf{E}\left[(Z_{n+1}^\beta - Z_n^\beta)(Z_1^\beta - Z_0^\beta)\right] - \mathbf{E}[Z_{n+1}^\beta - Z_n^\beta]\mathbf{E}[Z_1^\beta - Z_0^\beta] \\
&= \mathbf{E}Z_{n+1}^\beta Z_1^\beta - \mathbf{E}Z_n^\beta Z_1^\beta - \mathbf{E}Z_{n+1}^\beta Z_0^\beta + \mathbf{E}Z_n^\beta Z_0^\beta \\
&\overset{(4.8)}{=} \frac{1}{2\beta}\left[e^{-\beta n} - e^{-\beta(n-1)} - \left(e^{-\beta(n+1)} - e^{-\beta n}\right)\right] \\
&\overset{(4.9)}{=} -\frac{1}{2}\beta e^{\beta(2\theta_\beta - n - 1)}.
\end{aligned}$$

We can now see that

$$\sum_{n=1}^\infty |\gamma_{Z^\beta}(n)| = \frac{1}{2}\beta e^{(2\theta_\beta-1)\beta}\sum_{n=1}^\infty (e^{-\beta})^n = \frac{1}{2}\beta\frac{e^{2(\theta_\beta-1)\beta}}{1-e^{-\beta}} < \infty, \qquad \text{for all } \beta \in \mathbb{R}_{>0},$$

which implies $(Z_t^\beta)_{t\in\mathbb{R}_{\geqslant 0}}$ is short-range dependent for all $\beta \in \mathbb{R}_{>0}$ (Definition 2.4). Since the increments of $(Z_t^\beta)_{t\in\mathbb{R}_{\geqslant 0}}$ are pairwise jointly Gaussian, the limiting increments as $\beta \searrow 0$ and $\beta \to \infty$ will also be pairwise jointly Gaussian with covariances given by the limit of the covariances of the approaching sequence of increments. Thus, the limiting process as $\beta \searrow 0$ is short-range dependent because $\gamma_{Z^0}(n) = 0$ for all $n \in \mathbb{N}$. The limiting process as $\beta \to \infty$ is also short-range dependent, because

$$\lim_{\beta\to\infty} \gamma_{Z^\beta}(n) = \lim_{\beta\to\infty} -\frac{1}{2}\beta e^{\beta(2\theta_\beta - n-1)} = 0, \qquad \text{for all } n \in \mathbb{N}.$$

On the other hand, the autocovariance function for the increments of the integrand in $\overline{B}_t^H$, which we will denote $\gamma_{H,\beta}$ is, in the case $H \in (0, 1/2)$,

$$\begin{aligned}\gamma_{H,\beta}(n) &= \mathbf{E}\left[\beta^{-1/2-H}(Z^\beta_{n+1} - Z^\beta_n)\beta^{-1/2-H}(Z^\beta_1 - Z^\beta_0)\right] \\ &= \beta^{-2H-1}\gamma_{Z^\beta}(n) = -\frac{1}{2}\beta^{-2H}e^{\beta(2\theta_\beta-n-1)}.\end{aligned}$$

A longer calculation is required in the case $H \in (1/2, 1)$, but the resulting expression differs only by a factor of -1. That is,

$$|\gamma_{H,\beta}(n)| = \frac{1}{2}\beta^{-2H}e^{\beta(2\theta_\beta-n-1)}, \qquad \text{for all } H \in (0, 1/2) \cup (1/2, 1),\ \beta \in \mathbb{R}_{>0}.$$

It is easily checked that $\gamma_{H,\beta}$ is absolutely summable for all $\beta \in \mathbb{R}_{>0}$, so the process specified by the Muravlev integrand is short-range dependent for all such β. Similarly, the autocovariance $\gamma_{H,\beta}(n) \to 0$ as $\beta \to \infty$ for all $n \in \mathbb{N}$, so the corresponding limiting process is also short-range dependent. However,

$$\lim_{\beta\searrow 0} |\gamma_{H,\beta}(n)| = \infty, \qquad \text{for all } H \in (0, 1/2) \cup (1/2, 1),\ n \in \mathbb{N},$$

so the limiting process will be long-range dependent for all such H.

These calculations suggest that the long-range dependence of the Muravlev integral representation of fBm originates from the portion of the integral near $\beta = 0$. This fits with intuition, because such β correspond to Ornstein-Uhlenbeck processes $(Z^\beta_t)_{t\in\mathbb{R}_{\geqslant 0}}$ which have only small speeds of mean reversion. In contrast, for large β, the processes $(Z^\beta_t)_{t\in\mathbb{R}_{\geqslant 0}}$ experience much stronger mean-reversion, and so will 'forget' their past more rapidly.

Of course, fBm is only long-range dependent for $H \in (1/2, 1)$, so the extra weight given to the processes $(Z^\beta_t)_{t\in\mathbb{R}_{\geqslant 0}}$ with small β parameters by the factor of $\beta^{-1/2-H}$ in the Muravlev representation appears to play a crucial role in determining whether the integral process $(\overline{B}^H_t)_{t\in\mathbb{R}_{\geqslant 0}}$ displays long-range dependence. However, it is not clear how to compute the autocovariance function $\gamma_{\overline{B}^H}$.

Existing approximation schemes for fBm often fail to capture long-range dependence (see, for instance, [8, Sec. 2.2.3]). If the long-range dependence of the Muravlev representation for $H \in (1/2, 1)$ can indeed be isolated to the portion of the integral near $\beta = 0$, then it may be possible to construct a process approximating fBm which displays the correct long-range dependence behaviour by using the truncated interval

$$\overline{c}_H \int_0^b \beta^{-1/2-H}(Z^\beta_t - Z^\beta_0 - B_t)\, d\beta, \qquad \text{for some } b \in \mathbb{R}_{>0}.$$

Chapter 5

Helix transformations

Using the general definition of a helix stated in [23, Ch. 10.5], a fractional Brownian motion can be viewed as a helix in L^2. This fact is not new — Kolmogorov acknowledged it by referring to fBm as the 'Wiener spiral' [25]. Nonetheless, it provides useful geometric intuition for the process. In this chapter we demonstrate that the transformation of an fBm from one Hurst parameter to another can be viewed as a manipulation of this helix.

Definition 5.1 (helix)**.** Let $\mathcal{H}$ be a real or complex Hilbert space and $X : [0, \infty) \to \mathcal{H}$ be a parametrised curve in $\mathcal{H}$. We say X is a *helix* in $\mathcal{H}$ if for all s,$t \in [0, \infty)$,

$$\|X(t) - X(s)\|_{\mathcal{H}}^2 = \psi(|t - s|),$$

for some function ψ. That is, if $\|X(t) - X(s)\|_{\mathcal{H}}$ depends only on $|t - s|$. The function ψ is called the *screw function*.

Definition 5.2 (helical process)**.** A *helical process* is a stochastic process which is a helix in L^2.

Since $\|B_t^H - B_s^H\|_{L^2} = \sqrt{\mathbf{E}|B_t^H - B_s^H|^2} = |t - s|^H$, the fBm $(B_t^H)_{t\geqslant 0}$ is a helical process with screw function $\psi(\cdot) = \cdot^{2H}$.

By definition, a process is helical if and only if it has weakly stationary increments. The form of the screw function can play a role in determining other distributional properties. For example, in the context of Gaussian processes, we have the following theorem.

Theorem 5.1. *Let $(X_t)_{t\geqslant 0}$ be a Gaussian helical process with mean zero and $X_0 = 0$. The process X_t is self-similar if and only if its screw function $\psi_X(\tau) = a\tau^b$ for some $a, b \in \mathbb{R}_{>0}$.*

Proof. First assume $(X_t)_{t\geqslant 0}$ is self similar. Then for arbitrary $c \in \mathbb{R}_{>0}$, $s, t \in \mathbb{R}_{\geqslant 0}$,

$$\psi_X^2(c(t - s)) = \mathbf{E}[(X_{ct} - X_{cs})^2] = \mathbf{E}[(c^b X_t - c^b X_s)^2] = c^{2b}\psi_X^2(t - s),$$

and taking $t - s = 1$ we see that $\psi_X(c) = \psi_X(1)c^b$, the required form.

The reverse direction follows because, assuming the screw function has the required form, we have

$$\begin{aligned}\mathbf{E}[(X_{ct} - X_{cs})^2] &= \psi_X^2(c(t - s)) \\ &= c^{2b}a^2(t - s)^{2b} \\ &= c^{2b}\psi_X^2(t - s) = \mathbf{E}[(c^b X_t - c^b X_s)^2].\end{aligned}$$

Now take $s = 0$, and use the polarisation identity together with the weakly stationary increments property that $\mathbf{E}[(X_t - X_s)^2] = \mathbf{E}[X_{t-s}^2]$ to recover the covariance functions for $(X_{ct})_{t\in\mathbb{R}_{\geqslant 0}}$ and $(c^b X_t)_{t\in\mathbb{R}_{\geqslant 0}}$. That they are the same, together with the fact that both are mean-zero Gaussian processes, implies $(X_{ct})_{t\in\mathbb{R}_{\geqslant 0}} \overset{d}{=} (c^b X_t)_{t\in\mathbb{R}_{\geqslant 0}}$, so $(X_t)_{t\in\mathbb{R}_{\geqslant 0}}$ is self-similar. □

Though proved independently, the above theorem is a variation on the result that a self-similar Gaussian process with stationary increments is an fBm, see [52, Def. 2.6.2].

Further discussion of helices in the context of stochastic processes can be found in Masani [33], along with references to earlier work by Wiener, Schoenberg, von Neumann and Kolmogorov.

5.1 Discrete time

In this section we review how the increments of an fBm with Hurst parameter H may be transformed into the increments of an fBm with Hurst parameter $K \neq H$ by using the Cholesky decomposition of relevant covariance matrices, and then prove that this transformation is equivalent to geometrically manipulating a discretised helix.

5.1.1 Transformation via Cholesky factors

We say a matrix $L = [\ell_{k,j}]_{k,j=1}^n \in \mathbb{R}^{n\times n}$ is *lower triangular* if all entries strictly above the major diagonal are zero. That is, if $\ell_{k,j} = 0$ for all $k < j$. The set of elements corresponding to $k \geqslant j$ are the *lower triangular elements*. Recall the following theorem.

Theorem 5.2 (Cholesky decomposition). *If matrix $A \in \mathbb{R}^{n\times n}$ is symmetric and positive definite, then there exists a unique lower triangular matrix $L \in \mathbb{R}^{n\times n}$ with positive diagonal entries such that $A = LL'$.*

A proof can be found in [14, Thm. 4.2.7]. If $A = [a_{k,j}]_{k,j=1}^n$, the elements of its Cholesky factor $L = [\ell_{kj}]_{k,j=1}^n$ can be computed using the following two formulae.

$$\ell_{k,k} = \sqrt{a_{k,k} - \sum_{i=1}^{k-1} \ell_{k,i}^2}, \qquad \text{for } k \in \mathbb{N}_{\leqslant n}, \tag{5.1}$$

$$\ell_{k,j} = \frac{1}{\ell_{j,j}} \left(a_{k,j} - \sum_{i=1}^{j-1} \ell_{k,i}\ell_{j,i} \right), \qquad \text{for } j \in \mathbb{N}_{<k}. \tag{5.2}$$

Two rudimentary algorithms are based on these formulae [44, Sec. 3.1.5]. The Cholesky-Crout algorithm first computes $L_{1,1}$ and proceeds column-by-column, the Cholesky-Banachiewicz algorithm also starts at $L_{1,1}$ but proceeds row-by-row. Due to the large number of square root operations required, both algorithms are quite slow. However, in the context of decomposing the covariance matrix of a random vector of fbm increments, we will see that they have an elegant geometric interpretation.

Theorem 5.3. *Let $H \in (0,1)$, and the random vector $\boldsymbol{B}^H$ be the first n adjacent length-Δ increments of an H-fBm. That is, for an H-fBm $(B_t^H)_{t\in\mathbb{R}_{\geqslant 0}}$,*

$$\boldsymbol{B}^H = \left(\boldsymbol{B}^H_{(1)}, \ldots, \boldsymbol{B}^H_{(n)}\right)' := \left(B^H_{k\Delta} - B^H_{(k-1)\Delta}\right)_{k=1}^n.$$

Choose any $K \in (0,1) \setminus \{H\}$. There exists a lower triangular matrix $L_{K\leftarrow H}$ such that the elements of $L_{K\leftarrow H}\boldsymbol{B}^H \overset{d}{=} \boldsymbol{B}^K$ are the corresponding increments of a K-fBm.

Proof. We will construct $L_{K\leftarrow H}$. The vector $\boldsymbol{B}^H$ is a multivariate normal random vector with mean $\mathbf{0}_n$ and covariance matrix $\Sigma_H = [\sigma_H^2(k,j)]_{k,j=1}^n$, where

$$\begin{aligned}\sigma_H^2(k,j) &= \mathbf{E}\left[\boldsymbol{B}^H_{(k)}\boldsymbol{B}^H_{(j)}\right] \\ &= \frac{\Delta^{2H}}{2}\left(|k-j-1|^{2H} + |k-j+1|^{2H} - 2|k-j|^{2H}\right)\end{aligned}$$

is the covariance for the increments described. From the Mandelbrot-van Ness representation of fBm in terms of standard Bm, it can be seen that no linear combination of the elements of $\boldsymbol{B}^H$ will be degenerate, because each of the disjoint increments of B_t^H can be written as a sum which includes noise term which is independent of all preceding increments. Thus, Σ_H will be non-singular and (strictly) positive definite.

Let $\boldsymbol{Z} \sim \mathrm{MVN}(\mathbf{0}_n, I_n)$ and $L_{H\leftarrow \boldsymbol{Z}}$ be the Cholesky decomposition of Σ_H. Then it holds that $\boldsymbol{B}^H \overset{d}{=} L_{H\leftarrow \boldsymbol{Z}}\boldsymbol{Z}$. Recall that the determinant of a lower triangular matrix is the product of the entries on its major diagonal, and that the inverse of a non-singular lower triangular matrix is also lower triangular. By Theorem 5.2, $L_{H\leftarrow \boldsymbol{Z}}$ has positive diagonal entries, so has lower triangular inverse $L_{\boldsymbol{Z}\leftarrow H} := L^{-1}_{H\leftarrow \boldsymbol{Z}}$. Finally let $L_{K\leftarrow \boldsymbol{Z}}$ be the Cholesky decomposition of Σ_K. Then

$$L_{K\leftarrow \boldsymbol{Z}}L_{\boldsymbol{Z}\leftarrow H}\boldsymbol{B}^H \overset{d}{=} L_{K\leftarrow \boldsymbol{Z}}L_{\boldsymbol{Z}\leftarrow H}L_{H\leftarrow \boldsymbol{Z}}\boldsymbol{Z} = L_{K\leftarrow \boldsymbol{Z}}\boldsymbol{Z} \overset{d}{=} \boldsymbol{B}^K$$

so $L_{K\leftarrow H} := L_{K\leftarrow \boldsymbol{Z}}L_{\boldsymbol{Z}\leftarrow H}$ is the desired matrix. □

Discretised helices

Due to the fractal nature of fBm sample paths, they cannot be simulated with perfect resolution but only on a finite set of time parameter values. What helical properties are preserved in such a discrete-time process?

The angle in L^2 between two random variables X and Y is the inverse cosine of their correlation, because the identity $\langle \boldsymbol{x}, \boldsymbol{y}\rangle = \|\boldsymbol{x}\|\|\boldsymbol{y}\|\cos\theta$ yields

$$\theta_{L^2}(X,Y) := \arccos\left(\frac{\langle X, Y\rangle_{L^2}}{\|X\|_{L^2}\|Y\|_{L^2}}\right) = \arccos\left(\frac{\mathbf{E}XY}{\sqrt{\mathbf{E}X^2\mathbf{E}Y^2}}\right).$$

Let $(X_t)_{t\geqslant 0}$ be a mean-zero Gaussian, self-similar helical process with $X_0 = 0$. Observe X_t at discrete times $\{k\Delta\}_{k\in\mathbb{N}}$ for some $\Delta > 0$. From Theorem 5.1 and the polarisation identity we see that

$$\begin{aligned}\mathbf{E}X_sX_t &= \frac{1}{2}\left(\mathbf{E}X_s^2 + \mathbf{E}X_t^2 - \mathbf{E}(X_t - X_s)^2\right) \\ &= \frac{a^2}{2}\left(s^{2b} + t^{2b} - |t-s|^{2b}\right).\end{aligned} \tag{5.3}$$

Thus the covariance between the observed increments

$$\begin{aligned}\mathbf{E}[(X_{k\Delta} - X_{(k-1)\Delta})(X_{j\Delta} - X_{(j-1)\Delta})] \\ &= \mathbf{E}X_{k\Delta}X_{j\Delta} - \mathbf{E}X_{k\Delta}X_{(j-1)\Delta} - \mathbf{E}X_{(k-1)\Delta}X_{j\Delta} + \mathbf{E}X_{(k-1)\Delta}X_{(j-1)\Delta} \\ &= \frac{a^2\Delta^{2b}}{2}\left(|k-j-1|^{2b} + |k-j+1|^{2b} - 2|k-j|^{2b}\right)\end{aligned} \tag{5.4}$$

depends only on the distance $|k-j|$, and consequently the L^2 angle between increments also depends only on $|k-j|$. Perhaps a discrete, self-similar, helical process can be characterised by the property that the L^2 angle between disjoint increments depends only on the time-distance between them.

All the assumptions in the above computations hold for fBm. Figure 5.1 shows how the angles between fBm increments vary as a function of the Hurst parameter H. Intuitively, disjoint increments are parallel for $H = 1$ and orthogonal at $H = 1/2$, but there is some subtle behaviour as $H \searrow 0$.

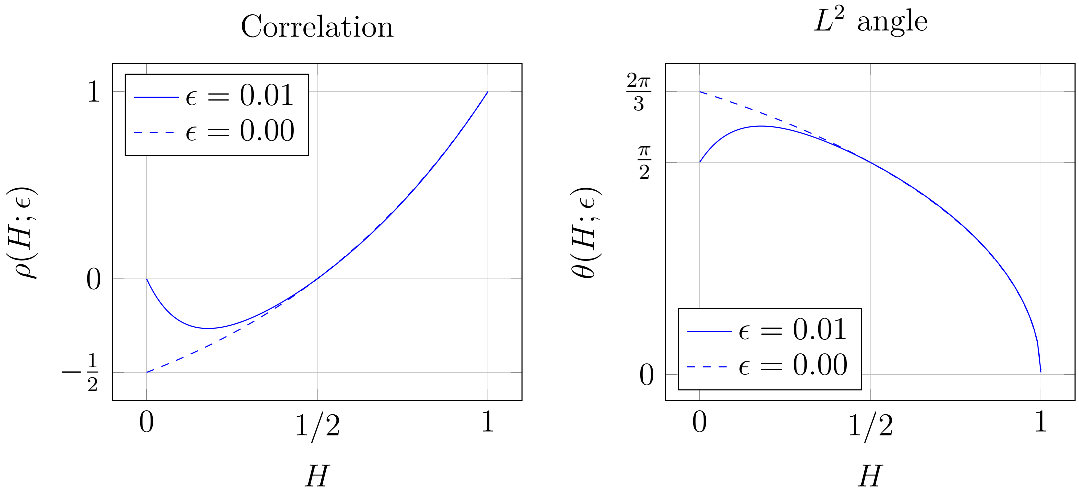

Figure 5.1: The correlation and L_2 angle between two increments of an H-fBm, as a function of H. The increments have unit length and are separated by distance ϵ. The relevant correlation is given by $\rho(H;\epsilon) = \frac{1}{2}\left(\epsilon^{2H} + (2+\epsilon)^{2H} - 2(1+\epsilon)^{2H}\right)$, and angle by $\theta(H;\epsilon) = \arccos\rho(H;\epsilon)$. Note that not all correlations $\rho \in [-1,1]$ can be obtained, and for the $\epsilon = 0$ case, when the increments share an end point, $\rho \nrightarrow 0$ as $H \searrow 0$.

To transform the increments $\boldsymbol{B}^H$ of an H-fBm into those of a K-fBm, we will see that it is sufficient to rotate all the increments in L^2 such that all pairwise L^2-angles are as required for increments of a K-fBm, and then rescale the increments so that each has the required L^2-norm (standard deviation). The following definitions, taken from [19, Def. 1.2,1.18], establish a structure that will facilitate this transformation.

Definition 5.3 (Gaussian Hilbert space)**.** A linear subspace $\mathcal{G}$ of $L^2_{\mathbb{R}}(\Omega, \mathcal{F}, \mathbf{P})$ is a *Gaussian inner product space* if each element of $\mathcal{G}$ is Gaussian and has mean zero. If $\mathcal{G}$ is complete, it is called a *Gaussian Hilbert space.*

Remark. The closure in L^2 of every Gaussian inner product space is a Gaussian Hilbert space, so we will only work with Gaussian Hilbert spaces hereafter.

Definition 5.4. A *Gaussian Hilbert space indexed by a (real) Hilbert space* $\mathcal{H}$ is a Gaussian Hilbert space $\mathcal{G}$ together with a specific linear isometry $\xi : \mathcal{H} \to \mathcal{G}$ which maps $h \mapsto \xi_h$.

For our purposes, we take $\mathcal{G}^n = \overline{\mathsf{span}(\{Z_1, \dots, Z_n\})}$ to be our Gaussian Hilbert space, where $\boldsymbol{Z} = (Z_1, \dots, Z_n)' \sim \text{MVN}(\mathbf{0}_n, I_n)$, and $\overline{\mathsf{span}(\dots)}$ denotes the closure of the linear span of a set of vectors. The space $\mathcal{G}^n$ can be indexed by $\mathbb{R}^n$, with the isometry $\xi : \mathbb{R}^n \to \mathcal{G}^n$ given by

$$\xi_{(x_1,\dots,x_n)} := x_1 Z_1 + \cdots + x_n Z_n.$$

Remark. Since $Z_1, \dots, Z_n$ form an orthonormal basis of $\mathcal{G}^n$, each vector $\boldsymbol{x} \in \mathbb{R}^n$ is the coordinate vector for the corresponding random variable $\xi_{\boldsymbol{x}} \in \mathcal{G}^n$.

Isometries preserve angles, so instead of working with random variables in $\mathcal{G}^n$ we can instead work with their vector-valued indices in $\mathbb{R}^n$. This perspective allows us to reinterpret the Cholesky factor $L_{H \leftarrow \boldsymbol{Z}}$ found in proof of Theorem 5.3. Namely, the rows of this matrix are the coordinates of the increments of an H-fBm in $\mathcal{G}^n$.

Let $\mathsf{L}^n = [\mathsf{l}_{k,j}]_{k,j=1}^n \in \mathbb{R}^{n \times n}$ be a lower triangular matrix such that $\mathsf{l}_{k,j} = 1$ for all $k \geqslant j$. Then $\mathsf{L}^n L_{H \leftarrow \boldsymbol{Z}} \boldsymbol{Z}$ is a random vector of the values of an H-fBm on a grid $t = k\Delta$, for $k \in \mathbb{N}_{\leqslant n}$. Accordingly, the rows of $\mathsf{L}^n L_{H \leftarrow \boldsymbol{Z}}$ are the coordinates in $\mathcal{G}^n$ of the values an H-fBm takes on the same grid. The dimensionality n will be large for any reasonable approximation to a continuous-time fBm, so the discrete helix cannot be visualised directly. However, we can gain a sense for it by performing dimensionality reduction via *principal component analysis*. Briefly, the method used is:

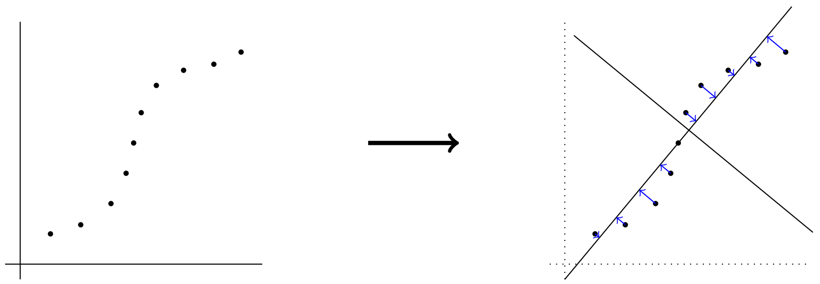

1° Treat the rows from the matrix $\mathsf{L}^n L_{H \leftarrow \boldsymbol{Z}}$ as a sample of points in $\mathbb{R}^n$. Subtract their mean to centre the sample.

2° Compute the normalised eigenvectors of the empirical covariance matrix of the sample.

3° Project the sample onto the 3-dimensional subspace spanned by eigenvectors corresponding to the three largest eigenvalues, ie. onto the three most significant principal components. The images of the points under this projection form a new sample in $\mathbb{R}^3$.

4° Plot the new sample, interpolating between points corresponding to adjacent points in the trajectory.

Figure 5.2 shows the result of this approach for $n = 1000$, $\Delta = 1/n$, and a range of Hurst parameter values.

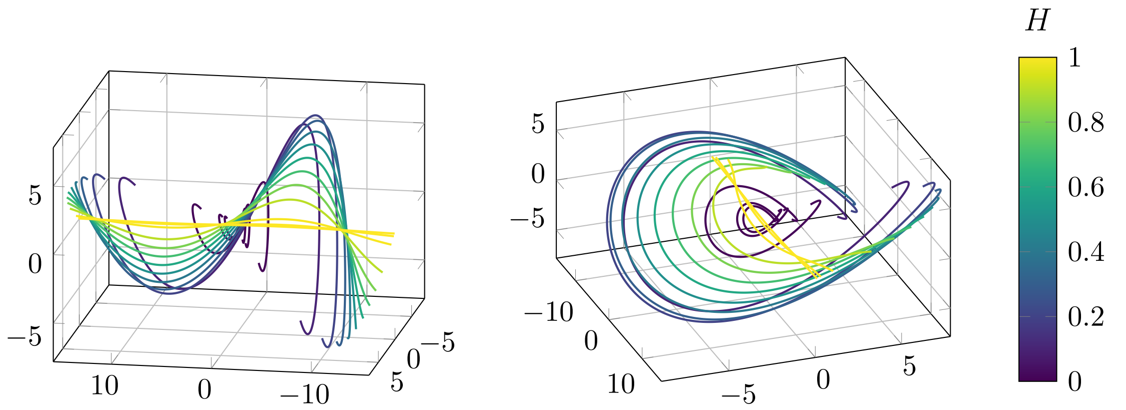

Figure 5.2: The projection onto the first three principal components of the sequence of elements in $\mathbb{R}^{1000}$ (the rows of $\mathsf{L}^n L_{H\leftarrow Z}$) that index the random process values in $\mathcal{G}^{1000}$ taken by an fBm at points $t = 0.001k$, for $k \in \mathbb{N}_{\leqslant 1000}$. Both plots are of the same objects, from different viewpoints. Curves are plotted for

$$H \in \{0.0001, 0.001, 0.01, 0.1, 0.2, 0.3, 0.4, 0.5, 0.6, 0.7, 0.8, 0.9, 0.99, 0.999, 0.9999\}.$$

All sequences of indices for $H \ll 1$ show helical structure. The helix becomes more tightly coiled as $H \searrow 0$—corresponding to obtuse angles between increments when $H \in (0, 1/2)$—and relaxes into a line as $H \nearrow 1$—corresponding astute (and decreasing) angles between increments for such H.

5.1.2 Transformation via helix manipulation

Given that each Cholesky factor in the proof of Theorem 5.3 is unique, it follows that a geometric approach—where each increment of an H-fBm is sequentially rotated and rescaled such that the resulting random vector forms the increments of a K-fBm—must produce the same result. Here we give a more precise statement and explicit proof of this fact.

Let $\mathring{L}_{K\leftarrow H} \in \mathbb{R}^{n\times n}$ be the linear transformation representing the above-described geometric procedure.

Theorem 5.4. *The matrix $\mathring{L}_{K\leftarrow H}$ is equal to $L_{K\leftarrow H}$, the matrix constructed in the proof of Theorem 5.3 via Cholesky factors.*

Proof. We will construct $\mathring{L}_{K\leftarrow H}$ ($\mathring{L}$, hereafter) by geometric arguments and show that it is equal to $L_{K\leftarrow H}$. Without loss of generality we can assume that $H = 1/2$, because all other cases can be constructed as the composition of a transformation of this form with the inverse of a transformation of this form.

Let $\boldsymbol{e}_1, \dots, \boldsymbol{e}_n$ be the standard orthonormal basis of $\mathbb{R}^n$ corresponding to our orthonormal basis $\xi_{\boldsymbol{e}_i} = Z_i$, $i \in \mathbb{N}_{\leqslant n}$ of $\mathcal{G}^n$. We wish to construct a matrix $\mathring{L}$ such that

$$\mathring{L}\boldsymbol{B}^{1/2} \overset{d}{=} \mathring{L}(\Delta^{1/2}\boldsymbol{Z}) \sim \mathrm{MVN}(\mathbf{0}_n, \Sigma_K).$$

The i-th element of the column vector $\Delta^{1/2}\boldsymbol{Z}$ is the element of $\mathcal{G}^n$ indexed by the vector $\Delta^{1/2}\boldsymbol{e}_i \in \mathbb{R}^n$. Since we are modifying each increment sequentially, based on conditions involving only the preceeding increments, $\mathring{L}$ will be lower-triangular, and we will construct it row by row. The setup is as follows.

Denote by $\boldsymbol{\ell}_i'$ the i-th row of $\mathring{L}$. Initialise $\mathring{L}_0 \in \mathbb{R}^{n\times n}$ to be the zero matrix. For $k \in \mathbb{N}_{\leqslant n}$, denote by $\mathring{L}_k$ the partially constructed matrix $\mathring{L}$ of the form

$$\mathring{L}_k = \left[\begin{array}{c|c} \Lambda_k & 0 \\ \hline 0 & 0 \end{array}\right] = \begin{bmatrix} \boldsymbol{\ell}_1' \\ \dots \\ \boldsymbol{\ell}_k' \\ \mathbf{0} \\ \dots \\ \mathbf{0} \end{bmatrix} \tag{5.5}$$

where $\Lambda_k \in \mathbb{R}^{k\times k}$ is a top-left square submatrix of $\mathring{L}$.

We require the vector $\Delta^{1/2}\boldsymbol{\ell}_k \in \mathbb{R}^n$ to be the vector index of the element of $\mathcal{G}^n$ which satisfies both $\|\xi_{\Delta^{1/2}\boldsymbol{\ell}_k}\|_{L^2} = \Delta^K$ and

$$\theta_{L^2}\left(\xi_{\Delta^{1/2}\boldsymbol{\ell}_i}, \xi_{\Delta^{1/2}\boldsymbol{\ell}_k}\right) = \arccos\left(\frac{\sigma_K^2(i,k)}{\sigma_K(i)\sigma_K(k)}\right), \qquad \text{for } i \in \mathbb{N}_{<k}. \tag{5.6}$$

But ξ is an isometry and $\sigma_K(i) = \Delta^K$ for all $i \in \mathbb{N}_{\leqslant n}$, so the conditions in (5.6) can be rewritten in terms of the standard Euclidean inner product as

$$\langle \boldsymbol{\ell}_i, \boldsymbol{\ell}_k \rangle = \frac{\sigma_K^2(i,k)}{\Delta}, \qquad \text{for } i \in \mathbb{N}_{<k}. \tag{5.7}$$

For $k = 1$, this condition is easily satisfied by setting $\boldsymbol{\ell}_1 = \Delta^{K-1/2}\boldsymbol{e}_1$. If we denote the elements of $\boldsymbol{\ell}_i$ by $\boldsymbol{\ell}_i = (\ell_{i,1}, \dots, \ell_{i,n})$, then, conditioned on knowing $\boldsymbol{\ell}_i$ for all $i \in \mathbb{N}_{<k}$, the elements $\ell_{k,1}, \dots, \ell_{k,k-1}$ of $\boldsymbol{\ell}_k$ can be calculated by solving the following system of linear equations which codifies the conditions (5.7):

$$\Lambda_k \begin{bmatrix} \ell_{k,1} \\ \dots \\ \ell_{k,k-1} \end{bmatrix} = \frac{1}{\Delta}\begin{bmatrix} \sigma_K^2(k,1) \\ \dots \\ \sigma_K^2(k,k-1) \end{bmatrix}.$$

Because Λ_k is lower triangular, the solutions have a recursive closed form given by

$$\ell_{k,j} = \frac{1}{\ell_{j,j}}\left(\frac{\sigma_K^2(k,j)}{\Delta} - \sum_{i=1}^{j-1}\ell_{k,i}\ell_{j,i}\right), \qquad \text{for } j \in \mathbb{N}_{<k},$$

and the diagonal element $\ell_{k,k}$ can then be calculated by

$$\ell_{k,k} = \sqrt{\frac{\sigma_K^2(k,k)}{\Delta} - \sum_{i=1}^{k-1}\ell_{k,i}^2}, \qquad \text{for } k \in \mathbb{N}_{\leqslant n},$$

which simply ensures that $\|\xi_{\Delta^{1/2}\boldsymbol{\ell}_k}\|_{L^2} = \Delta^K$. The second formula also works for our initial value of $\ell_{1,1}$. But then, these are exactly the standard formulae 5.1 and 5.2 used for computing the Cholesky decomposition of $\Delta^{-1}\Sigma_K$. Thus, $\mathring{L}$ is lower triangular and equal to the Cholesky decomposition of $\Delta^{-1}\Sigma_K$, or equivalently, $\mathring{L} = \Delta^{-1/2} L_{K\leftarrow \boldsymbol{Z}}$ where $L_{K\leftarrow \boldsymbol{Z}}$ is the Cholesky decomposition of Σ_K.

But by the construction of $L_{K\leftarrow 1/2}$ in the proof of Theorem 5.3, we know that

$$L_{K\leftarrow 1/2} = L_{K\leftarrow \boldsymbol{Z}} L_{\boldsymbol{Z}\leftarrow 1/2} = L_{K\leftarrow \boldsymbol{Z}}\left(\frac{1}{\Delta^{1/2}} I_n\right) = \frac{1}{\Delta^{1/2}} L_{K\leftarrow \boldsymbol{Z}}.$$

Thus $\mathring{L}_{K\leftarrow 1/2} = L_{K\leftarrow 1/2}$. □

5.2 Continuous time

It is plausible that the linear transformation described in the previous section may approach some limiting, continuous-time transformation as the spacing of the grid on which the fBm is discretised approaches zero. In this section, the discrete-time transformation developed in the previous section is numerically compared with the continuous-time Molchon-Golosov representation (Theorem 3.2), which has a similar structure.

Molchan-Golosov representation

Let $T \in \mathbb{R}_{>0}$ and $(B_t)_{t\in[0,T]}$ be a standard Bm on the compact time interval $[0,T]$. Recall that for $t \in [0,T]$, the Molchan-Golosov representation $(\widehat{B}^H_t)_{t\in[0,T]}$ of an H-fBm is given by

$$\widehat{B}^H_t = \int_0^t G_H(s,t)\, dB_s, \tag{5.8}$$

where the integrand

$$G_H(s,t) = \widehat{c}_H (t-s)^{H-1/2} {}_2F_1\left(1/2 - H, H - 1/2, H + 1/2, \frac{s-t}{s}\right)$$

depends only on the parameter of integration s and the upper terminal t. Thus (5.8) transforms a standard Bm on the compact time interval $[0,T]$ to an H-fBm on the same interval, and for every $t \in [0,T]$, the value B^H_t of the fBm depends only on $(B_s)_{s\in[0,t]}$. This is a 'lower triangular' structure similar that of the discrete-time transformation constructed using Cholesky factors in Theorem 5.3.

To compare the two, we need to discretise the integral process in (5.8). Taking $T = 1$, constants $n, m \in \mathbb{N}$ and $\Delta := 1/n$, we will use the following grid of points on the unit interval.

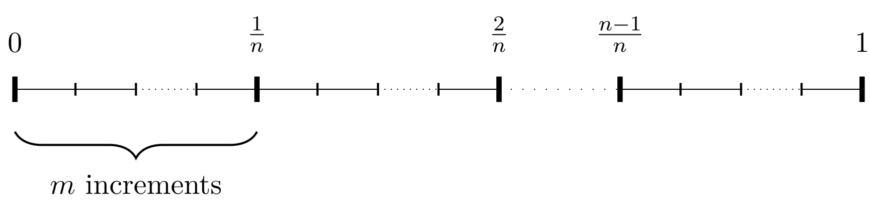

For the remainder of this thesis, we will assume that $(B_t)_{t\in\mathbb{R}_{\geqslant 0}}$ is the standard Bm driver of $(\widehat{B}_t^H)_{t\in\mathbb{R}_{>0}}$, and adopt the notation:

$$\widehat{\boldsymbol{B}}^H = \left(\widehat{B}^H_{k\Delta} - \widehat{B}^H_{(k-1)\Delta}\right)_{k=1}^{n}, \quad \text{and} \quad \boldsymbol{B} = \left(B_{j\Delta/m} - B_{(j-1)\Delta/m}\right)_{j=1}^{nm}.$$

Note that the increments $\boldsymbol{B}$ of the standard Bm are taken on a finer grid than those of the resulting integral transformation, $\widehat{\boldsymbol{B}}^H$. The Itô integral in equation 5.8 is defined as the limit of the Itô integrals of simple functions, so

$$\begin{aligned}
\widehat{\boldsymbol{B}}^H_{(k)} &= \int_0^{k\Delta} G_H(s, k\Delta)\, dB_s - \int_0^{(k-1)\Delta} G_H(s,(k-1)\Delta)\, dB_s \\
&\approx \sum_{j=1}^{km} G_H\Big(\frac{(j-1)\Delta}{m} + \frac{\Delta\delta_{j1}}{2m}, k\Delta\Big)\boldsymbol{B}_{(j)} \\
&\qquad\qquad - \sum_{j=1}^{(k-1)m} G_H\Big(\frac{(j-1)\Delta}{m} + \frac{\Delta\delta_{j1}}{2m}, (k-1)\Delta(k-1)\Big)\boldsymbol{B}_{(j)} \\
&= \sum_{j=1}^{km} \Big[G_H\Big(\frac{(j-1)\Delta}{m} + \frac{\Delta\delta_{j1}}{2m}, k\Delta\Big) \\
&\qquad\qquad - G_H\Big(\frac{(j-1)\Delta}{m} + \frac{\Delta\delta_{j1}}{2m}, (k-1)\Delta\Big)\mathbb{1}(j \leqslant (k-1)m)\Big]\boldsymbol{B}_{(j)},
\end{aligned}$$

and thus $\widehat{\boldsymbol{B}}^H$ can be approximated by a linear transformation of $\boldsymbol{B}$. Specifically, if we construct a matrix $\widehat{L}_{H\leftarrow 1/2} = [\widehat{\ell}_{k,j}]_{k\in\mathbb{N}_{\leqslant n}, j\in\mathbb{N}_{\leqslant mn}} \in \mathbb{R}^{n\times mn}$ such that

$$\begin{aligned}
\widehat{\ell}_{k,j} = \mathbb{1}(j \leqslant km)\Big[&G_H\Big(\frac{(j-1)\Delta}{m} + \frac{\Delta\delta_{j1}}{2m}, k\Delta\Big) \\
&- G_H\Big(\frac{(j-1)\Delta}{m} + \frac{\Delta\delta_{j1}}{2m}, (k-1)\Delta\Big)\mathbb{1}(j \leqslant (k-1)m)\Big], \\
&\qquad\qquad \text{for } k \in \mathbb{N}_{\leqslant n}, j \in \mathbb{N}_{\leqslant mn},
\end{aligned}$$

then $\widehat{\boldsymbol{B}}^H \approx \widehat{L}_{H\leftarrow 1/2}\boldsymbol{B}$. In the $m = 1$ case, $\widehat{L}_{H\leftarrow 1/2}$ is square, lower triangular, and analogous to the discrete time transformation matrix $L_{H\leftarrow 1/2}$.

The extra term $(\Delta\delta_{j1})/2m$, where δ_{j1} is Kronecker's delta, is required to avoid the case when the first parameter of G_H is zero, which would require division by zero. This inelegant fix means that the sum is no longer of the form used in the construction of the Itô integral, but because the extra term is only non-zero for $j = 1$, the discrepancy is negligible in the limit as $n \to \infty$.

5.2.1 Comparison of transformation matrices

In this section, we will assume that $m = 1$, so that the matrices $\widehat{L}_{H\leftarrow 1/2}$ and $L_{H\leftarrow 1/2}$ have the same dimensions. It does not appear easy to analytically compare the elements of these matrices. The elements of $L_{H\leftarrow 1/2}$ are defined recursively as functions of the elements of Σ_H via (5.1) and (5.2). In constrast, the elements of $\widehat{L}_{H\leftarrow 1/2}$ are defined as linear combinations of particular values of the Gauss hypergeometric function. Nonetheless, numerical investigations suggest that they appear to approach each other in the limit as $n \to \infty$.

Figure 5.3 and Table 5.1 describe the distribution of the absolute relative differences between the lower triangle (non-zero) matrix elements of $\widehat{L}_{H\leftarrow 1/2}$ and $L_{H\leftarrow 1/2}$ for several values of n and H. That is, for $\widehat{L}_{H\leftarrow 1/2} = [\widehat{\ell}_{k,j}]_{k,j=1}^{n}$ and $L_{H\leftarrow 1/2} = [\ell_{k,j}]_{k,j=1}^{n}$, the distribution of elements in the set

$$\left\{ \left| \frac{\ell_{k,j} - \widehat{\ell}_{k,j}}{\widehat{\ell}_{k,j}} \right| \text{ for } j,k \in \mathbb{N}_{\leqslant n} \text{ and } k \geqslant j \right\}.$$

We emphasise that the elements in such sets are deterministic.

For all H, both the mean and standard deviation this set of absolute relative differences between the non-zero elements of the two transformation matrices appears to approach zero as $n \to \infty$, though the convergence is faster for larger H.

5.2.2 Comparison of simulated paths

A second approach to comparing the transformation via Cholesky factors with the approximation to the Molchan-Golosov integral representation is to compare, for a given $\boldsymbol{B}$, their resulting trajectories. Allowing $\boldsymbol{B}$ to be random, we can then generate a sample of trajectory discrepancies.

In particular, we are interested in whether the approximate sample trajectories generated via the Cholesky factor method approach the ‘true’ H-fBm $\widehat{B}_t^H$ generated by the Molchan-Golosov representation.

It is not possible to simulate a Bm in continuous time, so we cannot compute the values taken by $\widehat{B}_t^H$ exactly. Nonetheless, since we are viewing it as a candidate for a limit, it is important that we approximate $\mathsf{L}^n \widehat{\boldsymbol{B}}^H$ as well as possible. Unfortunately, $\widehat{B}_t^H$ is a Volterra process—not an Itô process—because the integrand G_H depends on the upper terminal of integration t. As a consequence, standard approaches to approximating Itô integral processes, such as the Euler-Maruyama method, cannot be used.

A rudimentary approximation to $\mathsf{L}^n \widehat{\boldsymbol{B}}^H$ is given by

$$\mathsf{L}^n \widehat{L}_{H\leftarrow 1/2} \boldsymbol{B}.$$

Here, the $\widehat{L}_{H\leftarrow 1/2}$ has the dimensions $n \times nm$ and $\boldsymbol{B}$ has dimensions $nm \times 1$. We can improve the approximation by increasing m and, moreover, estimating the limiting value of the vector $\mathsf{L}^n \widehat{L}_{H\leftarrow 1/2} \boldsymbol{B}$ as $m \to \infty$.

Fix $m = 4$, and define the matrix

$$\mathsf{D}^{n\widetilde{m}} = [\mathsf{d}_{k,j}]_{k \in \mathbb{N}_{\leqslant n\widetilde{m}}, j \in \mathbb{N}_{\leqslant nm}} \in \mathbb{R}^{n\widetilde{m} \times nm}, \qquad \text{where } \mathsf{d}_{kj} = \mathbb{1}((k-1)\widetilde{m} < j \leqslant k\widetilde{m}),$$

to be a generalised diagonal matrix which ‘pools’ the increments in $\boldsymbol{B}$ such that $\mathsf{D}^{n\widetilde{m}} \boldsymbol{B}$ has dimensions $n\widetilde{m} \times 1$. Then, for a given $\boldsymbol{B}$, we can compute

$$\mathsf{L}^n \widehat{L}_{H\leftarrow 1/2}^{n,m_i} \mathsf{D}^{nm_i} \boldsymbol{B}, \qquad \text{for } m_i = 2^{i-1},\ i \in \mathbb{N}_{\leqslant 3},$$

a sequence of increasingly close approximations to $\mathsf{L}^n\widehat{\boldsymbol{B}}^H$ corresponding to $m_1 = 1$, $m_2 = 2$ and $m_3 = 4$. In the above expression, the transformation matrix $\widehat{L}^{n,m_i}_{H\leftarrow 1/2}$ is labelled with an m_i to make clear that it, too, depends both on n and m_i, the latter of which is substituted for m in the definition (5.2).

Using this length-3 sequence of approximations, we can employ Richardson's extrapolation to estimate the limit as $m_i \to \infty$. To do so, we assume that there exists an expression of the following form for each approximate process value of $\widehat{B}^H_t$ in the vector $\mathsf{L}^n\widehat{L}^{n,m_i}_{H\leftarrow 1/2}\mathsf{D}^{nm_i}\boldsymbol{B}$:

$$(\mathsf{L}^n\widehat{L}^{n,m_i}_{H\leftarrow 1/2}\mathsf{D}^{nm_i}\boldsymbol{B})_{(k)} = \widehat{B}^H_{k/n} + \frac{a_1}{m_i} + \frac{a_2}{m_i^2} + O(\frac{1}{m_i^3}), \qquad \text{for } m_i \in \mathbb{N}, k \in \mathbb{N}_{\leqslant n}. \quad (5.9)$$

Then, ignoring the asymptotic error term $O(1/m_i^3)$, we can solve the system of three linear equations described by (5.9) for the unknowns a_1, a_2 and $\widehat{B}^H_{k/n}$, the last of which gives an estimate $\widehat{B}^H_{k/n,\mathsf{Richardson}}$ for the true value $\widehat{B}^H_{k/n}$ which is approached as $m_i \to \infty$. The notation

$$\widehat{\boldsymbol{B}}^H_{\mathsf{R}} = (\widehat{B}^H_{k/n,\mathsf{Richardson}} - \widehat{B}^H_{(k-1)/n,\mathsf{Richardson}})^n_{k=1}, \qquad \widehat{B}^H_{0,\mathsf{Richardson}} := 0,$$

will be used to refer to the vector of the limiting increments.

It is not clear whether the assumption (5.9) holds, but in simulations the sequence of approximate trajectories constructed via Cholesky factors (details below) does appear to approach $\mathsf{L}^n\widehat{\boldsymbol{B}}^H_{\mathsf{R}}$ marginally more quickly than it does $\mathsf{L}^n\widehat{L}^{n,m}_{H\leftarrow 1/2}\boldsymbol{B}$.

Take $n = 1000$. Having constructed an approximation to $\mathsf{L}^n\widehat{\boldsymbol{B}}^H$, we can now set up the sequence of approximated trajectories computed using Cholesky factors that are speculated to approach it. In our simulations, these correspond to the sequence of vectors:

$$\mathsf{L}^{n_i}L^{n_i}_{H\leftarrow 1/2}\mathsf{D}^{n_i}\boldsymbol{B}, \qquad n_i = 125 \times 2^{i-1},\ i \in \mathbb{N}_{\leqslant 4}.$$

Each such vector gives the values of an H-fBm at a grid of n_i points within the unit interval, where $n_1 = 125$, $n_2 = 250$, $n_3 = 500$ and $n_4 = 1000$. The transformation $L^{n_i}_{H\leftarrow 1/2}$ is labelled with a n_i to make clear that it, too, depends on n_i, which is substituted for n in the construction given in the proof of Theorem 5.3. In other words, each vector $\mathsf{L}^{n_i}L^{n_i}_{H\leftarrow 1/2}\mathsf{D}^{n_i}\boldsymbol{B}$ gives the values of an H-fBm on the grid $t = k/n_i$, $k \in \mathbb{N}_{\leqslant n_i}$, constructed from the vector of Bm increments $\boldsymbol{B}$ using Cholesky factors.

Note that the length of this vector will be different for each n_i, so we will take the final element in each vector, corresponding to the value of an H-fBm at $t = 1$, to be the single point at which we compare trajectories. Differences in the size of each simulated increment tend to accumulate, so the discrepancy at $t = 1$ is generally the largest observed over the interval $t \in [0, 1]$.

Table 5.2 describes the distribution of the sets

$$\left\{|(\mathsf{L}^n\widehat{\boldsymbol{B}}^H_{\mathsf{R}})_{(n)} - (\mathsf{L}^{n_i}L^{n_i}_{H\leftarrow 1/2}\mathsf{D}^{n_i}\boldsymbol{B})_{n_i}| \text{ for 20 realisations of } \boldsymbol{B}\right\},$$

for a range of values of H and the sequence of n_i introduced above. That is, the distribution of absolute differences between the simulated value of an H-fBm at time

$t = 1$ transformed from $\boldsymbol{B}$ using the Cholesky method, and the approximate value of the $\widehat{B}_1^H$ driven by the same Bm.

For most values of H, both the mean and standard deviation of the absolute errors appear to decrease towards zero as the number of increments $n\nu_i$ increases, though convergence slows as H nears 0 or 1, and was not observable in samples of this size for $H \in \{0.01, 0.99\}$. Given that convergence can be seen for all other values of H, this lack of convergence appears likely to be an artefact of the relatively small sample size. The slowing of the rate of convergence as H diverges from $1/2$ may intuitively be expected due to the increased roughness of the process for H near 0 and, for H near 1, the fact that near-straight trajectories will tend to compound errors.

An example of the sample trajectories obtained using, respectively, the Cholesky transformation and the Richardson extrapolation approximation to the Molchan-Golosov integral, is presented in Figure 5.4, overlaid on the shared Bm driver.

These numerical results suggest that the discrete-time transformation via Cholesky factors converges to the continuous-time Molchan-Golosov integral representation, and thus that the analogous geometric intuition for the transformation (namely, the contortion of the fBm helix) applies in the continuous-time case.

Code used for the numerical results in this section can be found in the appendix.

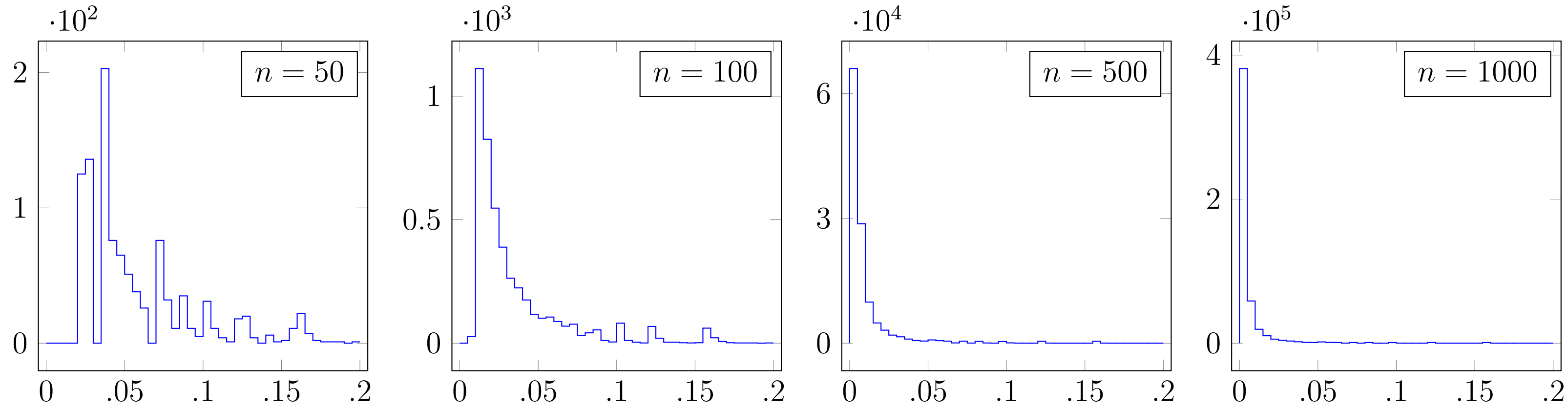

Figure 5.3: Distribution of relative absolute differences between the lower-triangle elements of $L_{H\leftarrow 1/2}$ and $\widehat{L}_{H\leftarrow 1/2}$, for increasing number of increments n. The distribution appears to approach a point mass at 0 as n increases.

H	$n = 50$	$n = 100$	$n = 500$	$n = 1000$	$n = 5000$
0.01	1.60×10^{0} (4.39×10^{0})	9.99×10^{-1} (3.17×10^{0})	3.64×10^{-1} (1.45×10^{0})	2.35×10^{-1} (1.03×10^{0})	8.00×10^{-2} (4.68×10^{-1})
0.1	3.48×10^{-1} (1.07×10^{0})	1.92×10^{-1} (7.72×10^{-1})	4.86×10^{-2} (3.52×10^{-1})	2.70×10^{-2} (2.49×10^{-1})	6.82×10^{-3} (1.12×10^{-1})
0.2	2.36×10^{-1} (6.02×10^{-1})	1.25×10^{-1} (4.41×10^{-1})	2.71×10^{-2} (2.03×10^{-1})	1.40×10^{-2} (1.44×10^{-1})	2.98×10^{-3} (6.47×10^{-2})
0.3	1.95×10^{-1} (4.09×10^{-1})	1.07×10^{-1} (3.04×10^{-1})	2.55×10^{-2} (1.42×10^{-1})	1.36×10^{-2} (1.01×10^{-1})	3.08×10^{-3} (4.56×10^{-2})
0.4	1.58×10^{-1} (3.11×10^{-1})	8.89×10^{-2} (2.33×10^{-1})	2.18×10^{-2} (1.10×10^{-1})	1.17×10^{-2} (7.86×10^{-2})	2.72×10^{-3} (3.54×10^{-2})
0.6	1.08×10^{-1} (2.24×10^{-1})	6.18×10^{-2} (1.69×10^{-1})	1.57×10^{-2} (8.03×10^{-2})	8.52×10^{-3} (5.74×10^{-2})	2.02×10^{-3} (2.59×10^{-2})
0.7	9.54×10^{-2} (2.04×10^{-1})	5.49×10^{-2} (1.54×10^{-1})	1.41×10^{-2} (7.36×10^{-2})	7.73×10^{-3} (5.26×10^{-2})	1.85×10^{-3} (2.38×10^{-2})
0.8	8.59×10^{-2} (1.91×10^{-1})	4.97×10^{-2} (1.45×10^{-1})	1.29×10^{-2} (6.96×10^{-2})	7.05×10^{-3} (4.98×10^{-2})	1.69×10^{-3} (2.25×10^{-2})
0.9	7.81×10^{-2} (1.81×10^{-1})	4.53×10^{-2} (1.39×10^{-1})	1.17×10^{-2} (6.72×10^{-2})	6.42×10^{-3} (4.81×10^{-2})	1.53×10^{-3} (2.18×10^{-2})
0.99	6.90×10^{-2} (1.79×10^{-1})	4.06×10^{-2} (1.33×10^{-1})	1.07×10^{-2} (6.51×10^{-2})	5.84×10^{-3} (4.69×10^{-2})	1.39×10^{-3} (2.14×10^{-2})

Table 5.1: Summary statistics for the distribution of the relative absolute errors between the lower triangle elements of $L_{H\leftarrow 1/2}$ and $\widehat{L}_{H\leftarrow 1/2}$. The first value stated is the mean of the relative absolute errors, the value in parentheses is their standard deviation. Both decrease as the number of increments into which the unit interval is subdivided (n) increases.

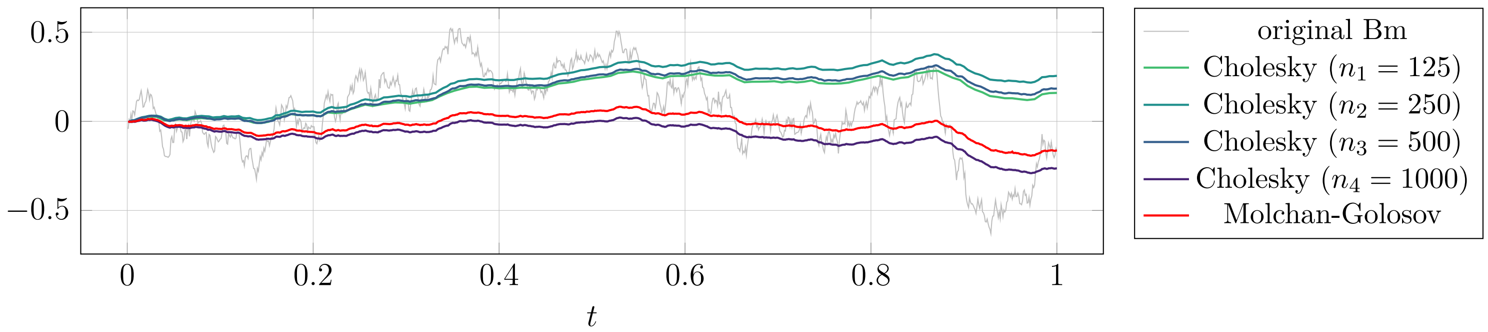

Figure 5.4: Simulated trajectories of a standard Bm and its transformations into an 0.9-fBm using (i) the discrete-time transformation via Cholesky factors, with values given by the elements of the vectors $\mathsf{L}^{n_i} L^{n_i}_{H\leftarrow 1/2} \mathsf{D}^{n_i} \boldsymbol{B}$ for $i \in \mathbb{N}_{\leqslant 4}$ and (ii) an approximation to the continuous-time Molchan-Golosov integral, with values given by the vector $\mathsf{L}^{n} \widehat{\boldsymbol{B}}^{H}_{\mathsf{R}}$. Convergence of the Cholesky method to the Molchan-Golosov integral is slow for H near 1, as can be seen here.

H	$n_1 = 125$	$n_2 = 250$	$n_3 = 500$	$n_4 = 1000$
0.01	5.15×10^{-1} (3.48×10^{-1})	6.52×10^{-1} (4.85×10^{-1})	5.41×10^{-1} (5.07×10^{-1})	5.01×10^{-1} (3.35×10^{-1})
0.1	2.55×10^{-1} (1.89×10^{-1})	2.53×10^{-1} (1.48×10^{-1})	2.08×10^{-1} (1.50×10^{-1})	1.66×10^{-1} (1.28×10^{-1})
0.2	1.16×10^{-1} (8.48×10^{-2})	1.17×10^{-1} (7.75×10^{-2})	9.75×10^{-2} (6.08×10^{-2})	7.25×10^{-2} (5.36×10^{-2})
0.3	5.45×10^{-2} (3.28×10^{-2})	4.63×10^{-2} (3.13×10^{-2})	3.24×10^{-2} (2.08×10^{-2})	1.87×10^{-2} (1.55×10^{-2})
0.4	1.28×10^{-2} (9.25×10^{-3})	7.72×10^{-3} (4.50×10^{-3})	5.17×10^{-3} (4.04×10^{-3})	4.21×10^{-3} (3.00×10^{-3})
0.6	7.83×10^{-3} (6.03×10^{-3})	6.16×10^{-3} (4.77×10^{-3})	4.28×10^{-3} (3.58×10^{-3})	3.21×10^{-3} (2.84×10^{-3})
0.7	3.77×10^{-2} (2.68×10^{-2})	3.17×10^{-2} (1.93×10^{-2})	2.42×10^{-2} (1.76×10^{-2})	1.28×10^{-2} (1.17×10^{-2})
0.8	9.33×10^{-2} (6.21×10^{-2})	7.85×10^{-2} (5.91×10^{-2})	6.28×10^{-2} (5.50×10^{-2})	5.40×10^{-2} (4.16×10^{-2})
0.9	2.85×10^{-1} (2.49×10^{-1})	2.17×10^{-1} (1.57×10^{-1})	1.86×10^{-1} (1.48×10^{-1})	1.57×10^{-1} (9.86×10^{-2})
0.99	7.42×10^{-1} (4.48×10^{-1})	5.41×10^{-1} (5.39×10^{-1})	7.19×10^{-1} (5.16×10^{-1})	6.56×10^{-1} (4.55×10^{-1})

Table 5.2: Summary statistics for the distribution of the absolute errors $|(\mathsf{L}^{n} \widehat{\boldsymbol{B}}^{H}_{\mathsf{R}})_{(n)} - (\mathsf{L}^{n_i} L^{n_i}_{H\leftarrow 1/2} \mathsf{D}^{n_i} \boldsymbol{B})_{n_i}|$ over a sample of 20 realisations of $\boldsymbol{B}$. The first value stated is the mean absolute error, the value in parentheses is the standard deviation. For all mid-range values of H, both decrease towards zero as the number of increments n_i increases.

Chapter 6

Conclusion

This thesis aimed to build insight into two integral representations of fractional Brownian motion.

First, the derivation of the Muravlev representation [43, Cor. 1] from the Mandelbrot-van Ness representation was presented in detail. The random Gaussian field Z_t^β appearing in the integrand was proven to be smooth in the β direction. A multivariate Ornstein-Uhlenbeck process was introduced and used to define transition probabilities for the $C(0,\infty)$-valued process $(Z_t)_{t\in\mathbb{R}_{\geqslant 0}}$ explicitly on cylindrical subsets of $C(0,\infty)$. The Kolmogorov extension theorem was used to extend the probability measures to the cylindrical σ-algebra. In this setting, we proved that $(Z_t^\cdot)_{t\in\mathbb{R}_{\geqslant 0}}$ satisfies the Markov property. Viewing the integrands in the Muravlev representation as stochastic processes in time, long-range dependence was shown to arise in the limit as $\beta \searrow 0$, but not as $\beta \to \infty$. Consequently, it was conjectured that one could construct an fBm approximation scheme based on the Muravlev representation that would exhibit long-range dependence by truncating the integral to the interval $[0,b]$ for some finite $b \in \mathbb{R}_{>0}$.

Second, the perspective of fBm as a helix in L^2 was introduced, and it was noted that the L^2-angles between disjoint increments of an H-fBm are acute for $H \in (0, 1/2)$ and obtuse for $H \in (1/2, 1)$. It was conjectured that, for $H, K \in (0,1)$, one could transform increments of an H-fBm to increments of a K-fBm by iteratively rotating and rescaling each increment in an appropriate space. Finite-dimensional Gaussian Hilbert spaces indexed by $\mathbb{R}^n$ were introduced for this purpose. It was shown that such a geometric procedure is mathematically equivalent to performing the same transformation of the random vector of increments via premultiplication by a lower-triangular matrix constructed using Cholesky factors, thus proving the conjecture. It was then observed that the Molchan-Golosov integral representation for fBm has an analogous lower-triangular structure. Numerical experiments suggested that the discrete-time transformation via Cholesky factors converges to the continuous-time Molchan-Golosov transformation, in terms of both the transformation operator and the resulting trajectories. Such convergence indicates that the Molchan-Golosov transformation can be understood geometrically as a constriction or relaxation of the fBm helix.

Appendix

Simulation of Z_t^β

A collection of Wolfram Language functions for the simulation of the random field Z_t^β from the Muravlev representation. These were used to generate the sample surface plotted in Figure 4.1.

```
CovarianceMatrix[min_, max_, step_] := Table[
   1 / (i + j),
   {i, min, max, step},
   {j, min, max, step}
  ];

ξ[min_, max_, step_] := RandomVariate[
    d = MultinormalDistribution[
      Table[0, Ceiling[(max - min) / step]],
      CovarianceMatrix[min + step, max, step]],
    1][[1]];

Plotξ[min_, max_, step_] := ListLinePlot[
   Transpose[{Range[min + step, max, step], ξ[min, max, step]}]
  ];

Z[{tmin_, tmax_, tstep_}, {bmin_, bmax_, bstep_}] := RandomFunction[
   ItoProcess[
    {-Range[bmin + bstep, bmax, bstep] *
      Table[z[i], {i, 1, Length[Range[bmin + bstep, bmax, bstep]]}],
     (* ⅆt coefficients *)
     Table[1, Length[Range[bmin + bstep, bmax, bstep]]]}, (* ⅆBt coefficients *)
    {Table[z[i], {i, 1, Length[Range[bmin + bstep, bmax, bstep]] }],
     ξ[bmin, bmax, bstep]}, (* state parameter, initial state *)
    t (* time parameter *)
   ],
   {tmin, tmax, tstep}
  ];
```

```
PlotZ[{tmin_, tmax_, tstep_}, {bmin_, bmax_, bstep_} ] := ListPlot3D[
   Flatten[
    Transpose[
       {Table[#[[1]], Length[Range[bmin + bstep, bmax, bstep]]],
        Range[bmin + bstep, bmax, bstep], #[[2]] }
      ] & /@ Normal[Z[{tmin, tmax, tstep}, {bmin, bmax, bstep}] ] [[1]],
    1],
   AxesLabel → {"t", "β", Subsuperscript[Z, t, β]},
   Mesh → None,
   PlotTheme -> "Monochrome",
   LabelStyle → Opacity[0]
  ];

ExportZ[{tmin_, tmax_, tstep_}, {bmin_, bmax_, bstep_}] := Export["Z.csv",
  N[Flatten[
    Transpose[
       {Table[#[[1]], Length[Range[bmin + bstep, bmax, bstep]]],
        Range[bmin + bstep, bmax, bstep], #[[2]] }
      ] & /@ Normal[Z[{tmin, tmax, tstep}, {bmin, bmax, bstep}] ] [[1]],
    1]],
  "csv"
 ]

Animateξ[{tmin_, tmax_, tstep_}, {bmin_, bmax_, bstep_}] := Animate[
   ListLinePlot[
    (Transpose[{Range[bmin + bstep, bmax, bstep], #[[2]]}] & /@
       Normal[Z[{tmin, tmax, tstep}, {bmin, bmax, bstep}] ][[1]]) [[
     Round[(t - tmin) / tstep] + 1]],
    PlotRange → {{bmin, bmax}, {-10, 10}}
   ],
   {t, tmin, tmax, tstep},
   AnimationRunning → False
  ];

Exportξ[{tmin_, tmax_, tstep_}, {bmin_, bmax_, bstep_}] := Export[
  "betawave.gif",
  Table[
   ListLinePlot[
    (Transpose[{Range[bmin + bstep, bmax, bstep], #[[2]]}] & /@
       Normal[Z[{tmin, tmax, tstep}, {bmin, bmax, bstep}] ][[1]]) [[n]],
    PlotRange → {{bmin, bmax}, {-10, 10}}] ,
   {n, 1, Length[Range[tmin, tmax, tstep]]}
  ]
]
```

Computation of helix transforms

A collection of Wolfram Language functions for the computation and simulation of the numerical results presented in Section 5.2.

The function `CholeskyIncrementTransform` returns $L^n_{H\leftarrow 1/2}$, `CholeskyIncrements` returns $L^n_{H\leftarrow 1/2}\mathsf{D}^n\boldsymbol{B}$, `CholeskyProcessTransform` returns $\mathsf{L}^n L^n_{H\leftarrow 1/2}$, and the function `CholeskyProcess` returns $\mathsf{L}^n L^n_{H\leftarrow 1/2}\mathsf{D}^n\boldsymbol{B}$. Analagously, `MgIncrementTransform` returns $\widehat{L}^{n,m}_{H\leftarrow 1/2}$, `MgProcess` returns $\mathsf{L}^n\widehat{L}^{n,m}_{H\leftarrow 1/2}\mathsf{D}^{nm}\boldsymbol{B}$ and `MgProcessRichardson` returns $\mathsf{L}^n\widehat{\boldsymbol{B}}^H_{\mathsf{R}}$.

```
#### covariance of fBm increments ####

R[i_, j_, Δ_, H_] := Δ^(2 H)/2 (Abs[i - j - 1]^(2 H) + Abs[i - j + 1]^(2 H) - 2 Abs[i - j]^(2 H))

IncrementCovariance[n_, Δ_, H_] := Table[R[i, j, Δ, H], {i, 1, n}, {j, 1, n}]


#### (standard) Brownian motion increments on [0,1] ####

BmIncrements[n_, Δ_] := RandomReal[NormalDistribution[0, Sqrt[Δ]], n]

PoolIncrements[B_, n_, m_, maxm_] :=
 Table[Sum[B[[i]], {i, (j - 1) * (maxm / m) + 1, j * (maxm / m)}], {j, 1, n * m}]


#### parameter setup ####

n = 1000;

ms = {1, 2, 4};

maxm = 4;

B = BmIncrements[n * maxm, N[1 / (n * maxm)]];

H = .8;


#### Cholesky transformation ####

CholeskyIncrementTransform[n_, H_] :=
 (N[Sqrt[n]]) * Transpose[CholeskyDecomposition[IncrementCovariance[n, N[1 / n], H]]]

CholeskyIncrements[n_, m_, maxm_, H_, B_] :=
 CholeskyIncrementTransform[n, H].PoolIncrements[B, n, m, maxm]

CholeskyProcessTransform[n_, H_] :=
 LowerTriangularize[Table[1, {i, 1, n}, {j, 1, n}]].CholeskyIncrementTransform[n, H]

CholeskyProcess[n_, m_, maxm_, H_, B_] :=
 CholeskyProcessTransform[n, H].PoolIncrements[B, n, m, maxm]
```

```
### Molchan-Golosov transformation ###

MgConstant[H_] := Sqrt[(2*H*Gamma[H + .5]*Gamma[1.5 - H])/Gamma[2 - 2 H]] * 1/Gamma[H + .5]

MgIntegrand[H_, s_, t_] := (t - s)^(H-.5) * Hypergeometric2F1[.5 - H, H - .5, H + .5, (s - t)/s]

MgCoeff[k_, j_, m_, Δ_, H_] := Piecewise[{{
    0,
    j > k*m
   }, {
    MgIntegrand[H, N[Δ/2], Δ*k*m],
    j == 1 && k == 1
   }, {
    MgIntegrand[H, N[Δ/2], Δ*k*m] - MgIntegrand[H, N[Δ/2], Δ*(k - 1)*m],
    j == 1 && k > 1
   }, {
    MgIntegrand[H, Δ*(j - 1), Δ*k*m],
    j > (k - 1)*m && j ≤ k*m
   }, {
    MgIntegrand[H, Δ*(j - 1), Δ*k*m] - MgIntegrand[H, Δ*(j - 1), Δ*(k - 1)*m],
    j ≤ (k - 1)*m
   }}]

MgIncrementTransform[n_, m_, H_] :=
 MgConstant[H]*Table[MgCoeff[k, j, m, N[1/(n*m)], H], {k, 1, n}, {j, 1, n*m}]

MgIncrements[n_, m_, maxm_, H_, B_] :=
 MgIncrementTransform[n, m, H].PoolIncrements[B, n, m, maxm]

MgProcessTransform[n_, m_, H_] :=
 LowerTriangularize[Table[1, {i, 1, n}, {j, 1, n}]].MgIncrementTransform[n, m, H]

MgProcess[n_, m_, maxm_, H_, B_] :=
 MgProcessTransform[n, m, H].PoolIncrements[B, n, m, maxm]

MgProcesses[n_, ms_, maxm_, H_, B_] :=
 Table[MgProcess[n, ms[[j]], maxm, H, B], {j, 1, Length[ms]}]

RichardsonMatrix[k_] := {
   {1, -1, -1},
   {1, -1/(2^k), -1/(2^(k + 1))},
   {1, -1/(4^k), -1/(4^(k + 1))}
  }

RichardsonLimit[seq_, k_] := LinearSolve[RichardsonMatrix[k], seq][[1]]

MgProcessRichardsonQuick[n_, seqs_, k_] :=
 Table[RichardsonLimit[seqs[[j]], k], {j, 1, n}]

MgProcessRichardson[n_, ms_, maxm_, H_, B_, k_] :=
 MgProcessRichardsonQuick[n, Transpose[MgProcesses[n, ms, maxm, H, B]], k]
```

Bibliography

[1] Arneodo, A., d'Aubenton Carafa, Y., Bacry, E., Graves, P., Muzy, J., and Thermes, C. Wavelet based fractal analysis of DNA sequences. *Physica D: Nonlinear Phenomena 96*, 1-4 (1996), 291–320.

[2] Bassingthwaighte, J. B., and Raymond, G. M. Evaluation of the dispersional analysis method for fractal time series. *Annals of Biomedical Engineering 23*, 4 (1995), 491–505.

[3] Borovkov, K., Mishura, Y., Novikov, A., and Zhitlukhin, M. Bounds for expected maxima of Gaussian processes and their discrete approximations. *Stochastics 89*, 1 (2017), 21–37.

[4] Carmona, P., Coutin, L., et al. Fractional Brownian motion and the Markov property. *Electronic Communications in Probability 3* (1998), 95–107.

[5] Carmona, P., Coutin, L., and Montseny, G. Approximation of some Gaussian processes. *Statistical Inference for Stochastic Processes 3*, 1-2 (2000), 161–171.

[6] Cutland, N. J., Kopp, P. E., and Willinger, W. Stock price returns and the Joseph effect: a fractional version of the Black-Scholes model. In *Seminar on Stochastic Analysis, Random Fields and Applications* (1995), Springer, pp. 327–351.

[7] Decreusefond, L., and Üstünel, A. S. Stochastic analysis of the fractional Brownian motion. *Potential Analysis 10*, 2 (1999), 177–214.

[8] Dieker, T. Simulation of fractional Brownian motion. *MSc Theses, University of Twente, Amsterdam, The Netherlands* (2004).

[9] Doob, J. L. *Stochastic processes*, vol. 101. New York Wiley, 1953.

[10] Dzhaparidze, K., and Van Zanten, H. A series expansion of fractional Brownian motion. *Probability Theory and Related Fields 130*, 1 (2004), 39–55.

[11] Dzhaparidze, K., Van Zanten, H., et al. Krein's spectral theory and the Paley–Wiener expansion for fractional Brownian motion. *The Annals of Probability 33*, 2 (2005), 620–644.

[12] Ernst, D., Hellmann, M., Köhler, J., and Weiss, M. Fractional Brownian motion in crowded fluids. *Soft Matter 8*, 18 (2012), 4886–4889.

[13] Folland, G. B. *Real analysis: modern techniques and their applications*, second ed. John Wiley & Sons, 1999.

[14] Golub, G. H., and Van Loan, C. F. *Matrix computations*, fourth ed. The Johns Hopkins University Press, 2013.

[15] Gonzalez Vivo, P., and Lowe, J. The book of shaders. `https://thebookofshaders.com/13/`, 2015. Accessed: 2019-02-14.

[16] Gushchin, A. A., and Küchler, U. On recovery of a measure from its symmetrization. *Theory of Probability & its Applications 49*, 2 (2005), 323–333.

[17] Harms, P. Strong convergence rates for Markovian representations of fractional Brownian motion, 2019.

[18] Harms, P., and Stefanovits, D. Affine representations of fractional processes with applications in mathematical finance. *Stochastic Processes and their Applications 129*, 4 (2019), 1185–1228.

[19] Janson, S. *Gaussian Hilbert spaces*, vol. 129. Cambridge University Press, 1997.

[20] Jost, C. Transformation formulas for fractional Brownian motion. *Stochastic Processes and their Applications 116*, 10 (2006), 1341–1357.

[21] Jost, C. *Integral transformations of Volterra Gaussian processes.* PhD thesis, University of Helsinki, 2007.

[22] Jost, C. On the connection between Molchan-Golosov and Mandelbrot-Van Ness representations of fractional Brownian motion. *The Journal of Integral Equations and Applications* (2008), 93–119.

[23] Kahane, J.-P. *Some random series of functions*, vol. 5. Cambridge University Press, 1993.

[24] Kolmogorov, A. N. Curves in Hilbert space which are invariant with respect to a one-parameter group of motions. *C.R. (Dokl.) Acad. Sci. USSR (N.S.) 26* (1940), 6–9. In English: Tikhomirov, V. M., ed. *Selected Works of A. N. Kolmogorov: Volume I: Mathematics and Mechanics.* Kluwer Academic Publishers, 1991.

[25] Kolmogorov, A. N. Wienersche spiralen und einige andere interessante kurven in hilbertscen raum. *C.R. (Dokl.) Acad. Sci. USSR (N.S.) 26* (1940), 115–118. In English: Tikhomirov, V. M., ed. *Selected Works of A. N. Kolmogorov: Volume I: Mathematics and Mechanics.* Kluwer Academic Publishers, 1991.

[26] Kordzakhia, N. E., Kutoyants, Y. A., Novikov, A. A., and Hin, L.-Y. On limit distributions of estimators in irregular statistical models and a new representation of fractional brownian motion. *Statistics & Probability Letters 139* (2018), 141–151.

[27] Kotz, S., Gikhman, I., and Skorokhod, A. *The Theory of Stochastic Processes II.* Classics in Mathematics. Springer Berlin Heidelberg, 2004.

[28] Lamperti, J. Semi-stable stochastic processes. *Transactions of the American Mathematical Society 104*, 1 (1962), 62–78.

[29] Liptser, R. S., and Shiryaev, A. N. *Statistics of random processes: I. General theory*, vol. 5. Springer Science & Business Media, 2013.

[30] Mandelbrot, B. B., and Van Ness, J. W. Fractional Brownian motions, fractional noises and applications. *SIAM Review 10*, 4 (1968), 422–437.

[31] Mandelbrot, B. B., and Wallis, J. R. Noah, Joseph, and operational hydrology. *Water Resources Research 4*, 5 (1968), 909–918.

[32] Marinucci, D., and Robinson, P. M. Alternative forms of fractional Brownian motion. *Journal of Statistical Planning and Inference 80*, 1-2 (1999), 111–122.

[33] Masani, P. On helixes in Hilbert space. i. *Theory of Probability & its Applications 17*, 1 (1972), 1–19.

[34] Masuda, H., et al. On multidimensional Ornstein-Uhlenbeck processes driven by a general Lévy process. *Bernoulli 10*, 1 (2004), 97–120.

[35] McKeague, I. W., and Sen, B. Fractals with point impact in functional linear regression. *Annals of Statistics 38*, 4 (2010), 2559.

[36] Meyer, Y., Sellan, F., and Taqqu, M. S. Wavelets, generalized white noise and fractional integration: the synthesis of fractional Brownian motion. *Journal of Fourier Analysis and Applications 5*, 5 (1999), 465–494.

[37] Mishura, Û. S. *Stochastic calculus for fractional Brownian motion and related processes*, vol. 1929. Springer Science & Business Media, 2008.

[38] Mishura, Y., and Valkeila, E. An extension of the Lévy characterization to fractional Brownian motion. *The Annals of Probability 39*, 2 (2011), 439–470.

[39] Molchan, G. M. Historical comments related to fractional Brownian motion. In *Theory and applications of long-range dependence*. Springer Science & Business Media, 2003, pp. 39–42.

[40] Molchan, G. M., and Golosov, Y. I. Gaussian stationary processes with asymptotically a power spectrum. In *Doklady Akademii Nauk* (1969), vol. 184, Russian Academy of Sciences, pp. 546–549.

[41] Molz, F. J., and Boman, G. K. A fractal-based stochastic interpolation scheme in subsurface hydrology. *Water Resources Research 29*, 11 (1993), 3769–3774.

[42] Mörters, P., and Peres, Y. *Brownian motion*, vol. 30. Cambridge University Press, 2010.

[43] Muravlev, A. A. Representation of a fractional Brownian motion in terms of an infinite-dimensional Ornstein-Uhlenbeck process. *Russian Mathematical Surveys 66*, 2 (2011), 439–441.

[44] Najm, F. N. *Circuit simulation*. John Wiley & Sons, 2010.

[45] Norros, I., Valkeila, E., and Virtamo, J. An elementary approach to a Girsanov formula and other analytical results on fractional Brownian motions. *Bernoulli 5*, 4 (1999), 571–587.

[46] Nourdin, I. *Selected aspects of fractional Brownian motion*, vol. 4. Springer, 2012.

[47] Øksendal, B. *Stochastic differential equations*. Springer, 2003.

[48] Perez, D. G., Zunino, L., and Glaravaglia, M. A fractional Brownian motion model for turbulent wave-front phase [atmospheric EM wave propagation]. In *Proceedings of the 2004 Asia-Pacific Radio Science Conference* (2004), IEEE, pp. 338–339.

[49] Pipiras, V., and Taqqu, M. S. Deconvolution of fractional Brownian motion. *Journal of Time Series Analysis 23*, 4 (2002), 487–501.

[50] Pipiras, V., and Taqqu, M. S. Fractional calculus and its connections to fractional Brownian motion. *Theory and applications of long-range dependence* (2003), 165–201.

[51] Pipiras, V., and Taqqu, M. S. Regularization and integral representations of Hermite processes. *Statistics & Probability Letters 80*, 23-24 (2010), 2014–2023.

[52] Pipiras, V., and Taqqu, M. S. *Long-range dependence and self-similarity*, vol. 45. Cambridge University Press, 2017.

[53] Protter, P. E. Stochastic integration and differential equations. In *Stochastic integration and differential equations*. Springer, 2005.

[54] Rowland, T., and Weisstein, E. W. Matrix exponential. From MathWorld—A Wolfram Web Resource. Accessed: 2019-05-05.

[55] Samoradnitsky, G. *Stable non-Gaussian random processes: stochastic models with infinite variance*. Routledge, 2017.

[56] Taqqu, M. S., et al. Benoît Mandelbrot and fractional Brownian motion. *Statistical Science 28*, 1 (2013), 131–134.

[57] Weisstein, E. W. Gamma function. From MathWorld—A Wolfram Web Resource. Accessed: 2019-05-15.

[58] Weisstein, E. W. Reflection relation. From MathWorld—A Wolfram Web Resource. Accessed: 2019-05-15.

[59] Williams, C. K., and Rasmussen, C. E. Gaussian processes for machine learning. *The MIT Press 2*, 3 (2006), 4.

[60] Yaskov, P. A maximal inequality for fractional Brownian motions. *Journal of Mathematical Analysis and Applications 472*, 1 (2019), 11–21.